

INTERTWINERS AND $A-D-E$ LATTICE MODELS

Paul A. Pearce¹ and Yu-kui Zhou²

*Mathematics Department, University of Melbourne,
Parkville, Victoria 3052, Australia*

Abstract

Intertwiners between $A-D-E$ lattice models are presented and the general theory developed. The intertwiners are discussed at three levels: at the level of the adjacency matrices, at the level of the cell calculus intertwining the face algebras and at the level of the row transfer matrices. A convenient graphical representation of the intertwining cells is introduced. The utility of the intertwining relations in studying the spectra of the $A-D-E$ models is emphasized. In particular, it is shown that the existence of an intertwiner implies that many eigenvalues of the $A-D-E$ row transfer matrices are exactly in common for a finite system and, consequently, that the corresponding central charges and scaling dimensions can be identified.

1 Introduction

The notion of intertwiners and cell calculus has been developed by many authors [1, 2, 3, 4] and is potentially very useful in studying two-dimensional lattice models. Here we continue the general development of intertwiners for critical $A-D-E$ lattice models, including the Temperley-Lieb [5, 6, 8, 9] and dilute [10, 11] models and point out the implications of these intertwining relations for the study of spectra.

The paper is organized as follows. In this section we define the critical $A-D-E$ lattice models and indicate how they are constructed from the adjacency matrices. In Section 2 we discuss the elementary intertwiners between the $A-D-E$ adjacency matrices. In Section 3 we present intertwiners at the level of the faces and discuss the cell calculus. In particular, we introduce cell graphs as a convenient graphical representation of the intertwining cells. In Section 4 we discuss intertwiners at the level of the row transfer matrices and indicate the consequences for the spectra of $A-D-E$ lattice models. Finally, in the Appendices, we give a comprehensive listing of the $A-D-E$ intertwiners and cells.

1.1 $A-D-E$ Lattice Models

The $A-D-E$ lattice models are interaction-round-a-face or IRF models [12] that generalize the restricted solid-on-solid (RSOS) models solved by Andrews, Baxter and Forrester [13] in 1984. At criticality, these models are given by solutions of the Yang-Baxter equation [14, 12] based on the Temperley-Lieb algebra and are associated with the classical

¹Email: pap@mundoe.maths.mu.oz.au

²Email: ykzhou@mundoe.maths.mu.oz.au

and affine A - D - E Dynkin diagrams [5, 6, 9] shown in Figure 1. States at adjacent sites of the square lattice must be adjacent on the Dynkin diagram. The face weights of faces not satisfying this adjacency condition for each pair of adjacent sites around a face vanish.

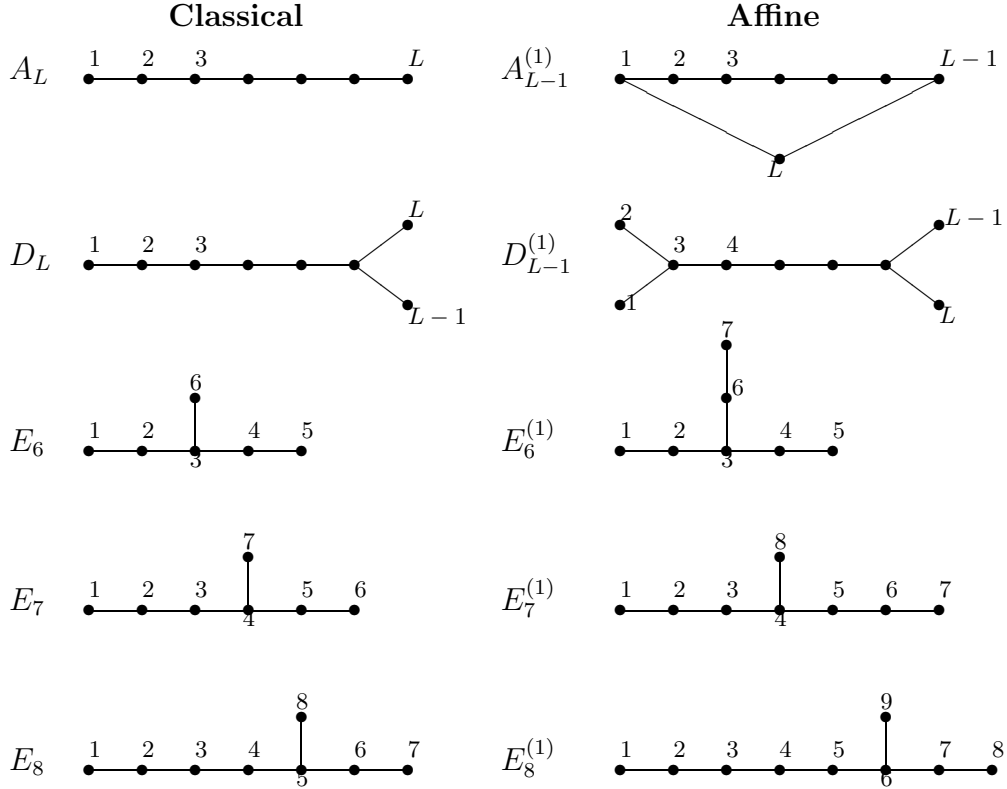


Figure 1. Dynkin diagrams of the classical and affine A - D - E Lie algebras

The face weights of the classical A - D - E models at criticality are given by [5]

$$W \left(\begin{array}{cc|c} d & c & u \\ a & b & \end{array} \right) = \frac{\sin(\lambda - u)}{\sin \lambda} \delta_{a,c} A_{a,b} A_{a,d} + \frac{\sin u}{\sin \lambda} \sqrt{\frac{S_a S_c}{S_b S_d}} \delta_{b,d} A_{a,b} A_{b,c} \quad (1.1)$$

where u is the spectral parameter and $\lambda = \pi/h$ is the crossing parameter. The Coxeter exponent h is given for each algebra in Table 1. The S_a are the positive components of the Perron-Frobenius eigenvector S of the adjacency matrix as given in Table 2. The adjacency matrix A has elements

$$A_{a,b} = \begin{cases} 1, & (a,b) \text{ adjacent} \\ 0, & \text{otherwise.} \end{cases} \quad (1.2)$$

The face weights of the affine $A_{L-1}^{(1)}$ and $D_{L-1}^{(1)}$ models [15, 16] at criticality can be written as

$$W \left(\begin{array}{cc|c} d & c & u \\ a & b & \end{array} \right) = \left[\frac{\sin(\lambda - u)}{\sin \lambda} \delta_{a,c} + \frac{\sin u}{\sin \lambda} \sqrt{\frac{S_a S_c}{S_b S_d}} \delta_{b,d} \right]$$

Lie algebra	h	m_j
A_L	$L + 1$	$1, 2, 3, \dots, L$
D_L	$2L - 2$	$1, 3, 5, \dots, 2L - 3, L - 1$
E_6	12	$1, 4, 5, 7, 8, 11$
E_7	18	$1, 5, 7, 9, 11, 13, 17,$
E_8	30	$1, 7, 11, 13, 17, 19, 23, 29$
$A_{L-1}^{(1)}$	L	$0, 2, 4, \dots, 2L - 2$
$D_{L-1}^{(1)}$	$2(L - 3)$	$0, 2, 4, \dots, 2(L - 3), L - 3, L - 3$
$E_6^{(1)}$	6	$0, 2, 2, 3, 4, 4, 6$
$E_7^{(1)}$	12	$0, 3, 4, 6, 6, 8, 9, 12$
$E_8^{(1)}$	30	$0, 6, 10, 12, 15, 18, 20, 24, 30$

Table 1. The Coxeter number h and the Coxeter exponents m_j for A - D - E classical and affine algebras.

Lie algebra	Perron-Frobenius Eigenvector
A_L	$\left(\sin \frac{\pi}{L+1}, \sin \frac{2\pi}{L+1}, \dots, \sin \frac{L\pi}{L+1}\right)$
D_L	$\left(2 \cos \frac{(L-2)\pi}{2L-2}, \dots, 2 \cos \frac{2\pi}{2L-2}, 2 \cos \frac{\pi}{2L-2}, 1, 1\right)$
E_6	$\left(\sin \frac{\pi}{12}, \sin \frac{\pi}{6}, \sin \frac{\pi}{4}, \sin \frac{\pi}{3} - \frac{\sin \frac{\pi}{4}}{2 \cos \frac{\pi}{12}}, \sin \frac{5\pi}{12} - \sin \frac{\pi}{4}, \frac{\sin \frac{\pi}{4}}{2 \cos \frac{\pi}{12}}\right)$
E_7	$\left(\sin \frac{\pi}{18}, \sin \frac{\pi}{9}, \sin \frac{\pi}{6}, \sin \frac{2\pi}{9}, \sin \frac{5\pi}{18} - \frac{\sin \frac{2\pi}{9}}{2 \cos \frac{\pi}{18}}, \sin \frac{\pi}{3} - \sin \frac{2\pi}{9}, \frac{\sin \frac{2\pi}{9}}{2 \cos \frac{\pi}{18}}\right)$
E_8	$\left(\sin \frac{\pi}{30}, \sin \frac{\pi}{15}, \sin \frac{\pi}{10}, \sin \frac{2\pi}{15}, \sin \frac{\pi}{6}, \sin \frac{\pi}{5} - \frac{\sin \frac{\pi}{6}}{2 \cos \frac{\pi}{30}}, \sin \frac{7\pi}{30} - \sin \frac{\pi}{6}, \frac{\sin \frac{\pi}{6}}{2 \cos \frac{\pi}{30}}\right)$
$A_{L-1}^{(1)}$	$(1, 1, \dots, 1)$
$D_{L-1}^{(1)}$	$(1, 1, 2, 2, \dots, 2, 2, 1, 1)$
$E_6^{(1)}$	$(1, 2, 3, 2, 1, 2, 1)$
$E_7^{(1)}$	$(1, 2, 3, 4, 3, 2, 1, 2)$
$E_8^{(1)}$	$(1, 2, 3, 4, 5, 6, 4, 2, 3)$

Table 2. The Perron-Frobenius eigenvectors for simply-laced classical and affine Lie algebras. The order of the components is fixed by the labelling of sites in the Dynkin diagrams of Figure 1. The corresponding eigenvalue is $\Lambda_{max} = 2$ for the affine algebras and $\Lambda_{max} = 2 \cos(\pi/h)$ for the classical algebras where the Coxeter number h is listed in Table 1.

$$+ \left(1 - \frac{\sin(\lambda - u)}{\sin \lambda} - \frac{\sin u}{\sin \lambda} \right) \sqrt{\frac{S_a}{S_b} \left(3 - \frac{S_a}{S_b} - \frac{S_b}{S_a} \right)} \bar{\delta}_{a,c} \bar{\delta}_{b,d} \left] A_{a,b} A_{b,c} A_{c,d} A_{d,a} \quad (1.3)$$

where the crossing parameter λ is arbitrary. For the affine A model, $\bar{\delta}$ is the usual Kronecker delta whereas, for the affine D model, $\bar{\delta}$ is modified to

$$\bar{\delta}_{a,b} = \bar{\delta}_{b,a} = \begin{cases} 1, & \text{if } a = b \\ 1, & \text{if } (a,b) = (1,2) \text{ or } (L-1,L) \\ 0, & \text{otherwise.} \end{cases} \quad (1.4)$$

The classical and affine A and D models admit off-critical elliptic extensions to the trigonometric solutions of the Yang-Baxter equations. This is not the case for the exceptional E models [7]. For the $A_{L-1}^{(1)}$ and $D_{L-1}^{(1)}$ models the elliptic extensions occur for $\lambda = s\pi/L$ and $\lambda = \pi/(L-3)$ respectively. There is as yet no known trigonometric solution to the Yang-Baxter equations for the IRF models whose adjacency conditions are given by the Dynkin diagrams of the exceptional affine Lie algebras $E_6^{(1)}$, $E_7^{(1)}$ and $E_8^{(1)}$. However, rational solutions are known [8] for all the affine A - D - E algebras

$$W \left(\begin{array}{cc|c} d & c & u \\ a & b & \end{array} \right) = \frac{\lambda - u}{\lambda} \delta_{a,c} A_{a,b} A_{a,d} + \frac{u}{\lambda} \sqrt{\frac{S_a S_c}{S_b S_d}} \delta_{b,d} A_{a,b} A_{b,c} \quad (1.5)$$

where λ is arbitrary.

The face weights of all the critical A - D - E models are invariant under the symmetries of the Dynkin diagrams and satisfy the crossing symmetry

$$W \left(\begin{array}{cc|c} d & c & u \\ a & b & \end{array} \right) = \sqrt{\frac{S_a S_c}{S_b S_d}} W \left(\begin{array}{cc|c} c & b & \lambda - u \\ d & a & \end{array} \right). \quad (1.6)$$

1.2 Dilute A - D - E Models

Recently, dilute A - D - E models were constructed [10, 11] by extending the methods of Pasquier [5] and Owczarek and Baxter [6]. These models allow adjacent sites on the lattice to be either in the same state or adjacent states on the Dynkin diagram. The face weights of the dilute A - D - E models are [10, 11]

$$\begin{aligned} W \left(\begin{array}{cc|c} d & c & u \\ a & b & \end{array} \right) &= \rho_1(u) \delta_{a,b,c,d} + \rho_2(u) \delta_{a,b,c} A_{a,d} + \rho_3(u) \delta_{a,c,d} A_{a,b} \\ &+ \sqrt{\frac{S_a}{S_b}} \rho_4(u) \delta_{b,c,d} A_{a,b} + \sqrt{\frac{S_c}{S_a}} \rho_5(u) \delta_{a,b,d} A_{a,c} + \rho_6(u) \delta_{a,b} \delta_{c,d} A_{a,c} \\ &+ \rho_7(u) \delta_{a,d} \delta_{c,b} A_{a,b} + \rho_8(u) \delta_{a,c} A_{a,b} A_{a,d} + \sqrt{\frac{S_a S_c}{S_b S_d}} \rho_9(u) \delta_{b,d} A_{a,b} A_{b,c} \end{aligned} \quad (1.7)$$

where the generalized Kronecker delta is 1 if all its arguments take the same value and is zero if its arguments are not the same value. The $A_{a,b}$ are elements of the adjacency matrix for the corresponding classical or affine Dynkin diagram of Figure 1. The weight

functions are

$$\begin{aligned}
\rho_1(u) &= \frac{\sin(2\lambda) \cos(3\lambda) + \sin u \cos(u + 3\lambda)}{\sin(2\lambda) \cos(3\lambda)}, & \rho_2(u) = \rho_3(u) &= \frac{\cos(u + 3\lambda)}{\cos(3\lambda)} \\
\rho_4(u) = \rho_5(u) &= \frac{\sin u}{\cos(3\lambda)}, & \rho_6(u) = \rho_7(u) &= \frac{\sin u \cos(u + 3\lambda)}{\sin(2\lambda) \cos(3\lambda)} \\
\rho_8(u) &= \frac{\sin(u + 2\lambda) \cos(u + 3\lambda)}{\sin(2\lambda) \cos(3\lambda)}, & \rho_9(u) &= \frac{\sin u \cos(u + \lambda)}{\sin(2\lambda) \cos(3\lambda)} \quad (1.8)
\end{aligned}$$

where the crossing parameter $\lambda = \frac{\pi}{4}(1 \pm \frac{1}{h})$. The dilute models admit an off-critical elliptic solution to the Yang-Baxter equations only for the classical A models.

2 Adjacency Matrix Intertwiners

Consider a connected graph such as one of the Dynkin diagrams in Figure 1. Each node of the graph is taken as a possible spin state for spins placed on the square lattice. States at adjacent sites of the square lattice must be adjacent on the graph. It turns out that there is a deep relation between two lattice models constructed in this way if an intertwiner can be constructed between them. The first indication of the existence of such an intertwiner is the existence of an intertwiner between the adjacency matrices of the two graphs. In this section we discuss intertwiners at the level of the adjacency matrices focusing on the A - D - E Dynkin diagrams. We will see that much of the theory of this section carries over, more or less directly, to the level of the row transfer matrices where the results and consequences are not so trivial.

Consider the adjacency matrices of the A - D - E Dynkin diagrams shown in Figure 1. It is straightforward to calculate the eigenvalues and orthonormalized eigenvectors. Remarkably, the adjacency matrix eigenvalues can all be written in the form $\Lambda_j = 2 \cos(m_j \pi/h)$ where the Coxeter number h and Coxeter exponents m_j are listed in Table 1. From the Perron-Frobenius theorem, it is known that such irreducible non-negative matrices possess a real and non-degenerate largest eigenvalue and that the corresponding Perron-Frobenius eigenvector S has all its components nonnegative. These Perron-Frobenius vectors are listed in Table 2 for the A - D - E adjacency matrices. The critical A - D - E models are constructed from these eigenstates as indicated in the previous section. The maximal eigenvalue Λ_{max} is a strictly increasing function of the matrix elements. It follows that the only connected graphs for which $\Lambda_{max} = 2$ are the Dynkin diagrams of the affine A - D - E Lie algebras. The allowed connected graphs for which $\Lambda_{max} < 2$ are the Dynkin diagrams of the classical A - D - E Lie algebras.

2.1 Properties of Intertwiners

Let A and G be adjacency matrices. In general, these are arbitrary square matrices with nonnegative integer elements. The adjacency matrix C is said to intertwine A and G if

$$AC = CG. \quad (2.1)$$

In general C is a rectangular matrix with nonnegative integer elements. It is easy to show that this intertwining relation

$$A \stackrel{\mathcal{C}}{\sim} G \tag{2.2}$$

is an equivalence relation acting on symmetric matrices, that is, it is (i) reflexive, (ii) symmetric and (iii) transitive:

$$\begin{aligned} \text{(i)} \quad & A \stackrel{I}{\sim} A \\ \text{(ii)} \quad & A \stackrel{\mathcal{C}}{\sim} G \text{ implies } G \stackrel{\mathcal{C}^T}{\sim} A \\ \text{(iii)} \quad & A \stackrel{\mathcal{C}}{\sim} B \text{ and } B \stackrel{\mathcal{C}'}{\sim} G \text{ implies } A \stackrel{\mathcal{C}\mathcal{C}'}{\sim} G. \end{aligned} \tag{2.3}$$

The existence of the intertwiner reflects a symmetry relating the two graphs associated with A and G . In particular, observe that the intertwining relation implies that

$$[CC^T, A] = [C^TC, G] = 0 \tag{2.4}$$

so that the symmetry operators CC^T and C^TC commute with A and G respectively and their eigenvalues can be used as quantum numbers labelling the eigenvectors of A and G .

The existence of an intertwiner also implies an overlap between the eigenvalues of A and G . Let us suppose that x is a simultaneous eigenvector of G and C^TC , that is,

$$Gx = \lambda x, \quad C^TCx = \mu x. \tag{2.5}$$

Then it follows from the intertwining relation that

$$A(Cx) = CGx = \lambda Cx \tag{2.6}$$

so that λ is an eigenvalue of A with eigenvector Cx provided that $Cx \neq 0$, or equivalently, $x^TC^TCx = \mu x^Tx \neq 0$. Hence Cx is an eigenvector of A provided x is not annihilated by the symmetry operator C^TC . Similarly, by the symmetry of the intertwining relation, it follows that if y is a simultaneous eigenvector of A and CC^T then C^Ty is an eigenvector of G provided y is not annihilated by the symmetry operator CC^T .

Note that if $x = S$ is the Perron-Frobenius eigenvector of G then, since C is nonnegative, Cx is a positive vector and is therefore the Perron-Frobenius eigenvector of A . Thus, if an intertwiner exists, the maximal eigenvalues of A and G are necessarily in common. Notice also that there is an intertwining relation between the symmetry operators CC^T and C^TC , namely,

$$CC^T \stackrel{\mathcal{C}}{\sim} C^TC. \tag{2.7}$$

It follows immediately from the previous considerations that all the nonzero eigenvalues of the symmetry operators CC^T and C^TC are in common. The properties of the symmetry operators are best understood by writing them in terms of fusion adjacency matrices. At first sight, this connection between intertwiners and fusion may seem surprising.

2.2 Adjacency Fusion Rules

The Temperley-Lieb A - D - E models are given by representations of the affine algebra $su(2)$. The higher-spin representations of this spin algebra are obtained by taking tensor products of the fundamental representation. The analog of this process for the A - D - E face models is fusion. Starting with a fundamental A , D or E solution of the Yang-Baxter equations it is possible to obtain a hierarchy of “higher-spin” solutions by fusing blocks of faces together. The fusion hierarchy of the classical A - D - E lattice models has been discussed by a number of authors [17, 18, 19, 20, 21]. At each fusion level n , a different adjacency condition is imposed on the states of the model. The adjacency matrices of these fused models are given by simple fusion rules.

Let A be the adjacency matrix of a classical or affine A - D - E Dynkin diagram. Then a fusion hierarchy of mutually commuting adjacency matrices $A^{(n)}$ is defined by the recursion relations

$$\begin{aligned} A^{(n)}A^{(1)} &= A^{(n-1)} + A^{(n+1)} \\ A^{(0)} &= I, \quad A^{(1)} = A \end{aligned} \tag{2.8}$$

where I is the identity matrix and $n = 1, 2, \dots$. For the classical A - D - E models these fusion rules close with $A^{(h-1)} = 0$ and

$$A^{(h-2)} = \begin{cases} I, & \text{for } D_L, E_7 \text{ and } E_8 \\ R, & \text{for } A_L \text{ and } E_6 \end{cases} \tag{2.9}$$

where h is the Coxeter number and R is the corresponding height reflection operator of the model defined as

$$R_{a,b} = \delta_{a,h-b}. \tag{2.10}$$

Using the adjacency intertwining relation (2.1) and the fusion rules it follows that the same intertwining relations hold between the fused adjacency matrices, that is,

$$A^{(n)}C = CA^{(n)}. \tag{2.11}$$

If we define the Chebyshev polynomials of the second kind $\mathcal{U}^{(n)}(z)$ by the same recursion (2.8) with $\mathcal{U}^{(0)}(z) = 1$ and $\mathcal{U}^{(1)}(z) = z$ then the eigenvalues of $A^{(n)}$ are given by

$$\Lambda_j^{(n)} = \mathcal{U}^{(n)}(2 \cos m_j). \tag{2.12}$$

The row transfer matrices of the fused classical A - D - E models also satisfy a fusion hierarchy [21]. Indeed, the matrices $A^{(n)}$ appearing in the above fusion rules are precisely the adjacency matrices for the level n fused models. In this way it is possible to obtain the adjacency matrices for all the fused A - D - E lattice models. Note that the fusion rules are also valid for the affine models but, in that case, the hierarchy is infinite with no closure.

2.3 Adjacency Intertwiners

The simplest example of an intertwiner relates the A and D Dynkin diagrams [3]. The A_L diagram possesses a \mathbb{Z}_2 symmetry corresponding to reflection about the midpoint of the

graph. For odd L , this symmetry can be used to construct an intertwiner with $D_{(L+3)/2}$ by an orbifold procedure [22]. Notice that the Dynkin diagrams A_L and $D_{(L+3)/2}$ have the same Coxeter number and hence the same maximal eigenvalue as required for the existence of an intertwiner. To obtain this intertwiner by the orbifold procedure, the nodes n and $L - n + 1$ of A are mapped to the node n' of D and the midpoint node $\frac{L+1}{2}$ of A is mapped to the two nodes $(\frac{L+1}{2})'$ and $(\overline{\frac{L+1}{2}})'$ of D . We can draw the graphs of A , D and the intertwiner C as in Figure 2. It is easy to check that the adjacency matrix

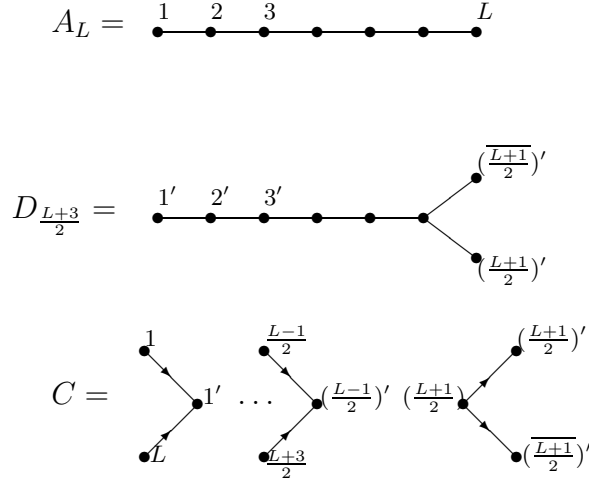


Figure 2. The graphs of A_L , $D_{(L+3)/2}$ and their intertwiner C . Notice that the edges of the graph of C are oriented as indicated by the arrows.

C for the A - D intertwiner obtained from the graph satisfies the intertwining relation $AC = CD$. The intertwining matrix C is listed explicitly in Appendix A. By direct matrix multiplication we see that the symmetry operators are given by

$$CC^T = (I + R_A), \quad C^T C = (I + R_D) \quad (2.13)$$

where the matrices R_A and R_D implement the \mathbb{Z}_2 symmetry on A and D respectively:

$$R_A = A^{(L-1)} = \begin{pmatrix} 0 & 0 & \dots & 0 & 1 \\ 0 & 0 & \dots & 1 & 0 \\ \vdots & \vdots & \ddots & \vdots & \vdots \\ 0 & 1 & \dots & 0 & 0 \\ 1 & 0 & \dots & 0 & 0 \end{pmatrix}, \quad R_D = \begin{pmatrix} 1 & 0 & \dots & 0 & 0 \\ 0 & 1 & \dots & 0 & 0 \\ \vdots & \vdots & \ddots & \vdots & \vdots \\ 0 & 0 & \dots & 0 & 1 \\ 0 & 0 & \dots & 1 & 0 \end{pmatrix} \quad (2.14)$$

Since R_A and R_D are involutions, the eigenvalues of the symmetry operators are $\mu = 0, 2$. Clearly, the eigenvalues of A and D with even eigenvectors ($\mu = 2$) under the \mathbb{Z}_2 symmetry will be in common and the eigenvalues with odd eigenvectors ($\mu = 0$) will not be in common. The eigenvalues of R_A are given by

$$r_A = \mathcal{U}^{(L-1)}(2 \cos m_j) = \begin{cases} 1, & m_j \text{ odd} \\ -1, & m_j \text{ even} \end{cases} \quad (2.15)$$

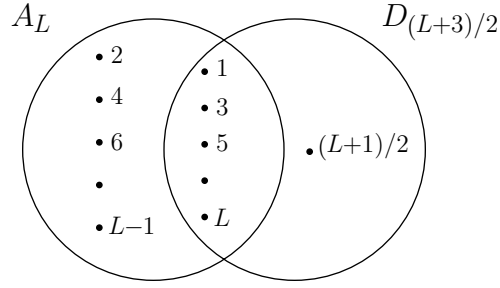


Figure 3. The overlap of the eigenvalues of A_L and $D_{(L+3)/2}$ labelled by the Coxeter exponents m_j . The common eigenvalues are even ($r_A = r_D = 1$) and the others are odd ($r_A, r_D = -1$) under the \mathbb{Z}_2 symmetry.

so the eigenvalues of A with odd Coxeter exponents are in common. The overlap of these eigenvalues and the labelling by quantum numbers is shown pictorially in Figure 3.

Intertwiners for all the adjacency matrices of the classical and affine A - D - E algebras are listed in Appendices A and B. The classical adjacency intertwiners were obtained previously by di Francesco and Zuber [4]. For the exceptional classical algebras we find

$$CC^T = \begin{cases} I + A^{(6)}, & \text{for } A_{11}-E_6 \\ I + A^{(8)} + A^{(16)}, & \text{for } A_{17}-E_7 \\ I + A^{(10)} + A^{(18)} + A^{(28)}, & \text{for } A_{29}-E_8 \end{cases} \quad (2.16)$$

$$C^TC = \begin{cases} I + E^{(6)}, & \text{for } A_{11}-E_6 \\ I + E^{(8)} + E^{(16)}, & \text{for } A_{17}-E_7 \\ I + E^{(10)} + E^{(18)} + E^{(28)}, & \text{for } A_{29}-E_8 \end{cases} \quad (2.17)$$

The eigenvalues of the symmetry operators can thus be written in terms of the polynomials $\mathcal{U}^{(n)}(2 \cos m_j)$. In each case they vanish except when m_j is a Coxeter exponent of $E_{6,7,8}$.

2.4 Intertwiners and Projectors

Loosely speaking, the action of intertwiners is to project onto the eigenspaces of the common eigenvalues. This suggests using projectors to construct the intertwiners. This is indeed possible. Let $|G|$ denote the number of vertices of G . The intertwining matrix C between A and G is then a $|A| \times |G|$ matrix. Let $|\psi^{(j)}\rangle$ denote the orthonormalized eigenvectors of A and $|\phi^{(j)}\rangle$ denote those of G . Then the combination of projectors

$$C = \sum_j c_j |\psi^{(j)}\rangle \langle \phi^{(j)}| \quad (2.18)$$

where c_j are coefficients and the summation is over the common eigenvalues (or equivalently the common Coxeter exponents) is a natural candidate for an intertwiner. In particular, it automatically satisfies the intertwining relation (2.1). But we require in addition that the matrix C has nonnegative integer elements. So care is needed to choose the coefficients c_j properly. A suitable choice [4] for the classical A - D and A - E

intertwiners is

$$C = \sum_j \frac{\phi_1^{(j)}}{\psi_1^{(j)}} |\psi^{(j)}\rangle \langle \phi^{(j)}|. \quad (2.19)$$

This choice gives the intertwiners listed in Appendix A.

The affine case is complicated by the occurrence of degenerate eigenvalues. Let us use subscripts to distinguish the vectors with the same Coxeter exponent in the case of degeneracy. The $A_{L-1}^{(1)}-D_{\frac{L}{2}+2}^{(1)}$ intertwiner can be obtained by the orbifold procedure and this gives the intertwiner

$$C = \begin{cases} \sqrt{2} \sum_{m=0}^{L/2} |\psi^{(2m)}\rangle \langle \phi^{(2m)}|, & L/2 \text{ odd} \\ \sqrt{2} \sum_{m=1}^{L/2} (1 - \delta_{m,L/4}) |\psi^{(2m)}\rangle \langle \phi^{(2m)}| + \sqrt{2} |\psi^{(L/2)}\rangle \langle \phi_1^{(L/2)}|, & L/2 \text{ even} \end{cases} \quad (2.20)$$

We have also found the coefficients c_j to obtain the adjacency matrix intertwiner for the affine $A-E$ cases. The adjacency matrix intertwiners for $A_5^{(1)}-E_6^{(1)}$, $A_7^{(1)}-E_7^{(1)}$ and $A_9^{(1)}-E_8^{(1)}$ are given respectively by

$$C = 2|\psi^{(0)}\rangle \langle \phi^{(0)}| + \sqrt{2}|\psi^{(2)}\rangle \langle \phi_1^{(2)}| + \sqrt{2}|\psi^{(4)}\rangle \langle \phi_1^{(4)}| + 2|\psi^{(6)}\rangle \langle \phi^{(6)}| \quad (2.21)$$

$$C = \sqrt{6}|\psi^{(0)}\rangle \langle \phi^{(0)}| + \sqrt{2}|\psi^{(2)}\rangle \langle \phi^{(3)}| + \sqrt{2}|\psi^{(4)}\rangle \langle \phi_1^{(6)}| + |\psi^{(6)}\rangle \langle \phi^{(9)}| + \sqrt{6}|\psi^{(8)}\rangle \langle \phi^{(12)}| \quad (2.22)$$

$$C = \sqrt{12}|\psi^{(0)}\rangle \langle \phi^{(0)}| + \sqrt{2}|\psi^{(2)}\rangle \langle \phi^{(6)}| + \sqrt{2}|\psi^{(4)}\rangle \langle \phi^{(12)}| + \sqrt{2}|\psi^{(6)}\rangle \langle \phi^{(18)}| + \sqrt{2}|\psi^{(8)}\rangle \langle \phi^{(24)}| + \sqrt{12}|\psi^{(10)}\rangle \langle \phi^{(30)}|. \quad (2.23)$$

Notice that the coefficients for the affine $A-G$ intertwiners are all $\sqrt{2}$ except the first and last which are given by

$$c_0 = \sqrt{\frac{\sum_i (S_i^G)^2}{h^A}}. \quad (2.24)$$

The Coxeter exponents m_j of the common eigenvalues can be simply read off from these formulas. In this way we obtain the adjacency matrices for the affine $A-D$ and $A-E$ intertwiners given in Appendix B.

3 Face Algebra and Cell Calculus

The face algebra of an $A-D-E$ model is generated by the face transfer operators $X_j(u)$. Let $a = \{a_1, a_2, \dots, a_N\}$ and $a' = \{a'_1, a'_1, \dots, a'_N\}$ be the configurations of two consecutive rows of spins of the lattice and apply periodic boundary conditions so that $a_{N+1} = a_1$ and $a'_{N+1} = a'_1$. Then the elements of the face transfer matrices $X_j(u)$ are given by

$$\langle a | X_j(u) | a' \rangle = W \left(\begin{array}{cc|c} a_{j-1} & a'_j & u \\ a_j & a'_{j+1} & \end{array} \right) \prod_{k \neq j} \delta(a_k, a'_k) = a_j \left\langle \begin{array}{c} a_{j-1} \\ \swarrow \quad \searrow \\ W \\ \nwarrow \quad \nearrow \\ a_{j+1} \end{array} \right\rangle a'_j \quad (3.1)$$

Notice that we have oriented the edges of the face with arrows. These are used for reference and must match the orientation of the bonds on the square lattice with all arrows pointing to the right or down. In terms of face transfer operators the Yang-Baxter equation takes the form

$$X_j(u)X_{j+1}(u+v)X_j(v) = X_{j+1}(v)X_j(u+v)X_{j+1}(u) \quad (3.2)$$

or graphically

$$= \quad (3.3)$$

and the inversion or unitarity condition is

$$X_j(u)X_j(-u) = \rho(u)\rho(-u)I. \quad (3.4)$$

In pictures the unitarity condition takes the form

$$= \rho(u)\rho(-u) \delta_{d,d'} \quad (3.5)$$

$$\frac{S_b S_d}{S_c S_a} = \rho(u)\rho(-u) \delta_{d,d'} \quad (3.6)$$

where I is the identity matrix, $\rho(u) = \sin(\lambda - u)/\sin \lambda$ and the second unitarity condition is obtained from the first by using the crossing symmetry. Taking the braided limits we obtain the braided matrices

$$b_j^{\pm 1} = \lim_{u \rightarrow \mp i\infty} \frac{X_j(u)}{\rho(u)} \quad (3.7)$$

which satisfy

$$b_{j+1}b_j b_{j+1} = b_j b_{j+1} b_j. \quad (3.8)$$

Consider two A - D - E models with intertwining adjacency matrices A and G and face weights W^A and W^G . Intertwiners between the face weights, or equivalently the two face algebras, can be obtained by constructing cells. This leads to the Ocneanu cell calculus [1, 3]. A cell is a face transfer operator C_j . The elements of the cell C_j are given by

$$\langle a | C_j(u) | a' \rangle = C \begin{pmatrix} a_{j-1} & a'_j \\ a_j & a_{j+1} \end{pmatrix} \prod_{k \neq j} \delta(a_k, a'_k) = a_j \begin{matrix} a_{j-1} \\ \swarrow \quad \searrow \\ a_j \quad a'_j \\ \nwarrow \quad \nearrow \\ a_{j+1} \end{matrix} \quad (3.9)$$

where

$$C \begin{pmatrix} d & c \\ a & b \end{pmatrix} = \begin{array}{ccc} & d & c_2 & c \\ & \downarrow & \rightarrow & \downarrow \\ g_1 & & & g_2 \\ & a & c_1 & b \end{array} \quad (3.10)$$

are a set of complex numbers which, in general, can depend on bond variables c_1, c_2, g_1, g_2 in addition to the spins a, b, c, d . Here the cells vanish unless the spins d, a are adjacent sites of A , the spins c, b are adjacent sites of G and the spins a, b and d, c are adjacent sites of the intertwining graph C . We adopt the convention that the value of a cell is changed into its complex conjugate after a reflection

$$\begin{array}{ccc} & d & c_2 & c \\ & \downarrow & \rightarrow & \downarrow \\ g_1 & & & g_2 \\ & a & c_1 & b \end{array} = \left(\begin{array}{ccc} & c & c_2 & d \\ & \downarrow & \rightarrow & \downarrow \\ g_2 & & & g_1 \\ & b & c_1 & a \end{array} \right)^* \quad (3.11)$$

We say that a cell system C_j intertwines the face weights W^A and W^G if

$$X_{j+1}^A C_j C_{j+1} = C_j C_{j+1} X_j^G \quad (3.12)$$

or graphically

$$\begin{array}{ccc} & a_{j-1} & & a_{j-1} \\ & \swarrow & & \swarrow \\ a_j & & W^A & & a'_j \\ & \searrow & & \searrow \\ & a_{j+1} & & a'_{j+1} \\ & \swarrow & & \swarrow \\ & a_{j+2} & & a_{j+2} \end{array} = \begin{array}{ccc} & a_{j-1} & & a_{j-1} \\ & \swarrow & & \swarrow \\ a_{j+1} & & & a'_j \\ & \searrow & & \searrow \\ & a_{j+2} & & a_{j+2} \\ & \swarrow & & \swarrow \\ & a_{j+2} & & a_{j+2} \end{array} \quad (3.13)$$

where for simplicity we have omitted the bond variables. We also require that the cells satisfy the unitarity conditions

$$\sum_{(b, c_1, g_2)} \begin{array}{ccc} & c & \\ & \swarrow & \swarrow \\ d & & g_2 & g_2 & c \\ & \searrow & & \searrow \\ & a & c_1 & c_1 & a \\ & \swarrow & & \swarrow \\ & a & & a \end{array} d' = \delta_{d, d'} \delta_{g_1, g_1'} \delta_{c_2, c_2'} \quad (3.14)$$

$$\sum_{(b, c_1, g_2)} \begin{array}{ccc} & c & \\ & \swarrow & \swarrow \\ d & & g_2 & g_2 & c \\ & \searrow & & \searrow \\ & a & c_1 & c_1 & a \\ & \swarrow & & \swarrow \\ & a & & a \end{array} d' \frac{S_b S_d}{S_c S_a} = \delta_{d, d'} \delta_{g_1, g_1'} \delta_{c_2, c_2'} \quad (3.15)$$

The cell intertwiner relation (3.12) and the two cell unitarity conditions (3.14) and (3.15) are analogues of the Yang-Baxter equation (3.2) and the usual unitarity conditions (3.5) and (3.6).

Once the intertwining relation (2.1) for the adjacency matrices is found, we can then construct the cell system satisfying the two unitary conditions and the intertwining relation for the face weights. There is a certain freedom amounting to a gauge freedom in the construction of the cells. For example, the phase angles of the cells can be changed such

that the two unitary conditions and the intertwining relation are still satisfied. Solving the two unitary conditions almost completely determines the cells but both the unitary conditions and the intertwining relation are needed to complete the determination. If the cells are found, the intertwining relation (3.12) tells us that the two models have the same integrability properties. In the following subsections it is shown that the cell systems for the classical A - D - E models are closely related to their corresponding adjacency matrices. In particular, the cells depend directly on the Perron-Frobenius eigenvectors of the graphs. We also give a systematic way to derive all the cells for intertwining relations of the classical and affine A - D - E models.

3.1 Classical A - D Cells

Let us first consider the cell calculus for the classical A - D models. Let A and D be the adjacency matrices of the A_L and $D_{\frac{L+3}{2}}$ models with odd L and suppose that $AC = CD$. We build the cells starting from the adjacency matrix C of the intertwiner. Consider the directed bonds (a, d) in C with $a \in A$ and $d \in D$. Two such edges (a, d) and (a', d') in C are considered to be adjacent if they form an allowed cell, that is, if a and a' are adjacent in A and d and d' are adjacent in D . In this way we represent a cell pictorially by projecting it onto two adjacent edges of C while maintaining the orientation

$$C \begin{pmatrix} a' & d' \\ a & d \end{pmatrix} = \begin{array}{ccc} a' & \xrightarrow{\quad} & d' \\ \downarrow & & \downarrow \\ a & \xrightarrow{\quad} & d \end{array} = \begin{array}{c} (a', d') \\ \bullet \\ \downarrow \\ \bullet \\ (a, d) \end{array} \quad (3.16)$$

The allowed cells are thus specified by an adjacency matrix or graph of adjacent edges of C .

The adjacency matrix intertwiner C is an L by $\frac{L+3}{2}$ rectangular matrix with the elements 0 or 1. The nonzero elements represent allowed edges (a, d) of C . Thus two nonzero elements are adjacent or neighbours if the row numbers of the elements are allowed nearest-neighbour pairs of the A -model and column numbers of the elements are allowed nearest-neighbour pairs of the D -model. We connect all of the neighbour elements with oriented bonds such that all arrows around one nonzero element go into or out of the element. Therefore we obtain two graphs from the adjacency matrix C of the intertwiner as pictured in Figure 4.

The oriented bonds in the two graphs of Figure 4 represent all of the allowed cells intertwining the classical A - D models. Each bond occurs twice with arrows in the opposite direction. So each bond corresponds to two different nonzero cells. We refer to the two graphs of Figure 4 as cell graphs. The cells in the two graphs of Figure 4 are independent of each other so we can consider these two graphs separately. There are only two classes of bonds in these graphs. We distinguish them as single bonds and face bonds. The latter ones form quadrilateral faces. Using the two unitarity conditions we find that the values of cells corresponding to the single bonds are independent and given by unimodular phase factors. In fact we can choose them to be 1. On the other hand, the cells corresponding to face bonds are involved in a set of dependent equations through the unitarity conditions. So to obtain the cells for face bonds, we initially satisfy just the

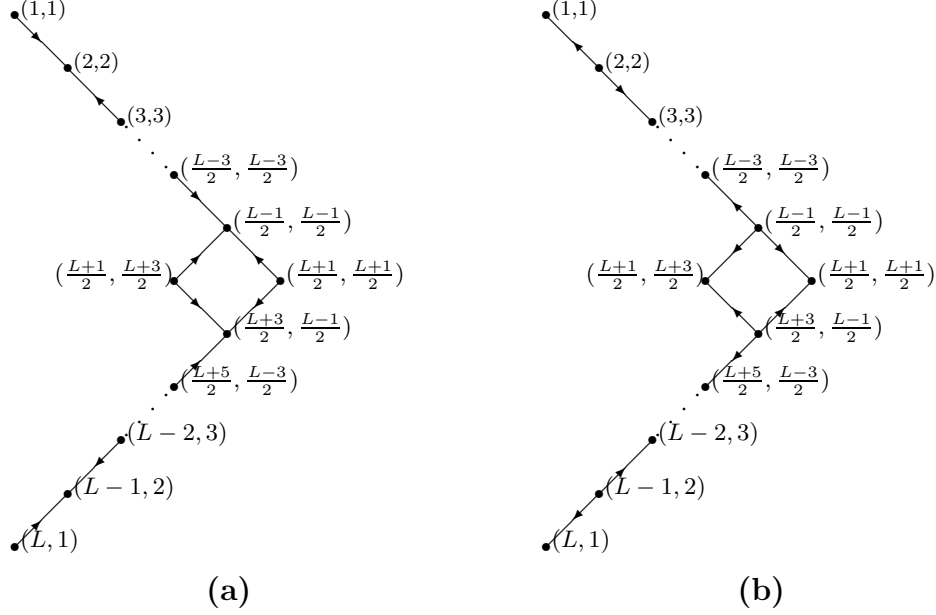


Figure 4. The cell graphs showing all the allowed cells intertwining the classical A - D models. The number of vertices in the graph is given by the number of nonzero elements of the adjacency intertwiner C .

first unitarity condition. The four cells on the face of Figure 4a, for example, are related to each other by the first unitarity condition and we can fix their values as

$$\begin{array}{c}
 \left(\frac{L-1}{2}, \frac{L-1}{2}\right) \\
 \swarrow \quad \searrow \\
 \left(\frac{L+1}{2}, \frac{L+3}{2}\right) \quad \left(\frac{L+1}{2}, \frac{L+1}{2}\right) \\
 \nwarrow \quad \nearrow \\
 \left(\frac{L+3}{2}, \frac{L-1}{2}\right)
 \end{array}
 =
 \begin{array}{c}
 -\sin m \quad \cos m \\
 \cos m \quad \sin m
 \end{array}
 \quad (3.17)$$

Obviously the values of these four cells satisfy the first unitarity condition for any angle m . They should also satisfy the equations from the second unitarity condition. So we can take one of these equations to fix the parameter m . For instance, from the normalization

$$\sin^2 m \frac{S_{(L+1)/2}^A S_{(L-1)/2}^D}{S_{(L+3)/2}^A S_{(L+1)/2}^D} = 1. \quad (3.18)$$

it follows that $m = \pi/4$.

In (3.17) we have chosen the cell

$$C \begin{pmatrix} (L+1)/2 & (L+3)/2 \\ (L-1)/2 & (L-1)/2 \end{pmatrix} = -\sin m \quad (3.19)$$

to be negative and all the others positive. We can change this to take any one of the four cells to be negative with the other three cells positive. Such choices also satisfy the unitarity conditions. The cells around the face in Figure 4a need only satisfy the first

unitarity condition and we can set them to 1 as we did for single bonds. But the four cells around the face of Figure 4b are related by the second unitarity condition. This is satisfied by taking only one of the four cells to be negative, say

$$\left(\frac{L+1}{2}, \frac{L+3}{2}\right) \longleftarrow \left(\frac{L-1}{2}, \frac{L-1}{2}\right) = -1. \quad (3.20)$$

Alternatively, this cell could be taken as 1 and the other three to be -1 . So we have derived all cells for the A - D models with odd L . These results are the same as those in [3]. The cells for the A - D models with even L can be taken as 1 because there are only single bonds in the cell graphs.

Lastly, we need to check that all of the cells satisfy the intertwining relations for the face weights of the A and D models. Notice that the faces in the cell graphs are of two types:

$$\text{Type A: } \begin{array}{c} \bullet \\ \swarrow \quad \searrow \\ \bullet \quad \bullet \\ \nwarrow \quad \nearrow \\ \bullet \end{array} \quad \text{or} \quad \text{Type B: } \begin{array}{c} \bullet \\ \swarrow \quad \searrow \\ \bullet \quad \bullet \\ \nwarrow \quad \nearrow \\ \bullet \end{array} \quad (3.21)$$

Using these we can summarize the rules to obtain the cells as follows:

1. The cells on single bonds are either 1 or -1 .
2. The absolute values of the cells on a face of type A are given by

$$\begin{array}{ccc} \sin m & \diamond & \cos m \\ \cos m & & \sin m \end{array} \quad (3.22)$$

One of these four cells should be negative and the other three positive. The angle m is $\pi/4$ if only one such face exists in the graph.

3. The absolute values of cells on isolated faces of type B are 1 and either one cell is negative and three are positive or one cell is positive and three are negative.

These rules determine the cells on single bonds and the absolute values of the cells on faces. The intertwining relation (3.12) can be used to determine which cells on faces are negative. In particular, it can be verified directly that the choice of the minus sign in (3.17) and (3.20) ensures that the intertwining relation of the A - D models is satisfied.

3.2 Classical A_{11} - E_6 and A_{17} - E_7 Cells

Now consider the A_{11} - E_6 intertwiner. In this case the adjacency matrix C given in Appendix A is a 12 by 6 matrix with the entries 0 or 1 [4]. We can derive the cell graphs of all allowed cells as we did for the A - D intertwiner. The result is shown in Figure 5.

This time there are five faces in each graph which we number from 1 to 5. Unlike the A - D models some face bonds are common to two faces. We divide the face bonds into two classes, shared face bonds and unshared face bonds. We need to augment the above rules to obtain cells on shared bonds. By studying the cell graphs in Figure 5 we see that the shared bonds always occur between a face of type A and a face of type B (see rules 2 and 3). The cells on a face of type A should be given by the rule 2 up to an angle m and a sign. To fix the angle m we introduce a new rule:

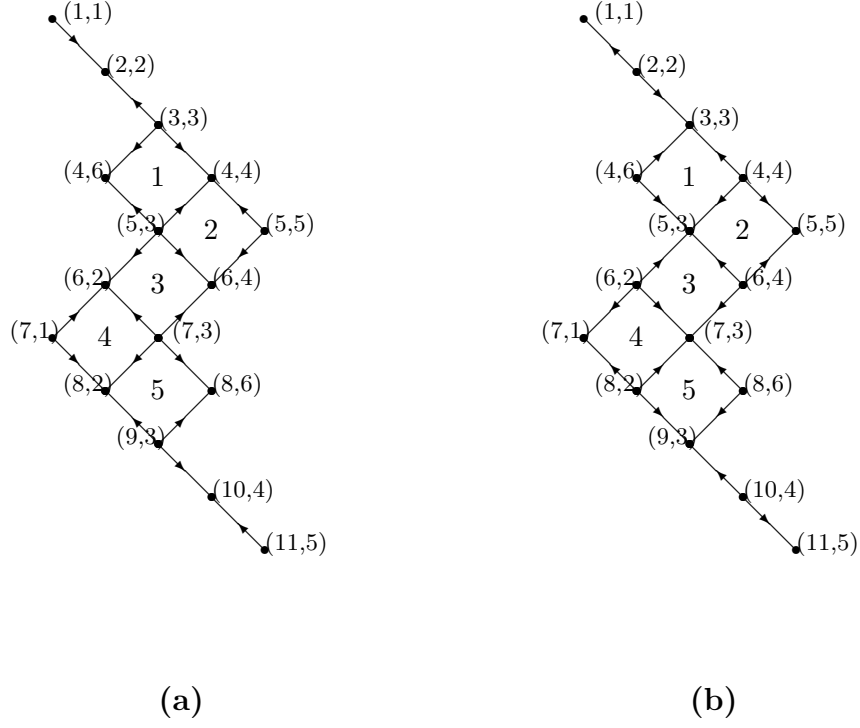


Figure 5. The cell graphs for the $A_{11}-E_6$ intertwiner.

4. The absolute value of the cell of a shared bond $(a,b) \longleftrightarrow (c,d)$ in a face of type B is related to the absolute value of the cell of the opposite bond in the face. Explicitly, if the opposite bond is $(a,b') \longleftrightarrow (c',d)$ then

$$\left| C \begin{pmatrix} c & d \\ a & b \end{pmatrix} \right| = \sqrt{\frac{S_{c'}^A S_{b'}^E}{S_c^A S_b^E}} \left| C \begin{pmatrix} c' & d \\ a & b' \end{pmatrix} \right| \quad (3.23)$$

The absolute values of cells of any unshared face bonds on a face of type B are 1. The absolute value of a cell of an unshared face bond $(a,b) \longleftrightarrow (c,d)$ on a face of type A is given by

$$\left| C \begin{pmatrix} d & c \\ a & b \end{pmatrix} \right| = \sqrt{\frac{S_a^A S_c^E}{S_d^A S_b^E}} \quad (3.24)$$

The values of the nonzero cells for the $A-E$ intertwiner are determined by these four rules up to some sign factors which are determined by the intertwining relation (3.12). It may happen that a face has two neighbouring faces and so there are two ways to find the absolute value of the cell on a shared bond. In such cases the two results always agree.

For example, applying rule 2 to face 4 in Figure 5a gives

$$\left| C \begin{pmatrix} 7 & 3 \\ 6 & 2 \end{pmatrix} \right| = \cos m_4. \quad (3.25)$$

Then rule 4 tells us that

$$\cos m_4 = \sqrt{\frac{S_5^A S_4^E}{S_7^A S_2^E}} \left| C \begin{pmatrix} 5 & 3 \\ 6 & 4 \end{pmatrix} \right| = \sqrt{\frac{S_5^A S_4^E}{S_7^A S_2^E}} \cos m_2 \quad (3.26)$$

from face 3 where, from face 1, we see that m_2 is given by

$$\left| C \begin{pmatrix} 5 & 3 \\ 4 & 4 \end{pmatrix} \right| = \sin m_2 = \sqrt{\frac{S_3^A S_6^E}{S_5^A S_4^E}}. \quad (3.27)$$

Also we get the same value of $|C(6, 2, 3, 7)|$ from face 5 by using

$$\sin m_4 = \sqrt{\frac{S_9^A S_6^E}{S_7^A S_2^E}} \quad (3.28)$$

and

$$\cos m_4 = \sqrt{1 - \sin^2 m_4} \quad (3.29)$$

We obtain the unshared bonds in face 4 and also

$$\left| C \begin{pmatrix} 7 & 3 \\ 6 & 2 \end{pmatrix} \right| = \left| C \begin{pmatrix} 7 & 1 \\ 8 & 2 \end{pmatrix} \right| = \cos m_4 = \sqrt{\frac{S_8^A S_1^E}{S_7^A S_2^E}} \quad (3.30)$$

which gives us the same value. Obviously it is simple to find the cell value $|C(6, 2, 3, 7)|$ from face 5 or from the unshared bond in face 4. Then we can show that this cell is negative, or $C(6, 2, 3, 7) = -|C(6, 2, 3, 7)|$, using the intertwining relation. Finally, because $\sin m_4 = \sin m_2$ we have $C(6, 2, 3, 7) = -\cos m_2$. In this way we can determine all of the cells completely for the $A_{11}-E_6$ intertwiner. The results are tabulated in Appendix C2.

The $A_{17}-E_7$ intertwiner can be obtained in a similar manner. The cell graphs for this intertwiner are shown in Figure 6. The derivation of the cells proceeds by applying the four rules as for the $A_{11}-E_6$ case. The results for the cells are tabulated in Appendix C3.

To summarize the procedure is (i) to draw the cell graphs from the adjacency matrix of the intertwiner, (ii) to obtain the absolute values of the cells by applying the four rules and then (iii) to fix the remaining sign factors using the full intertwining relations.

3.3 Classical $A_{29}-E_8$ Cells

Let us now consider the $A_{29}-E_8$ intertwiner. The cell graphs for the $A_{29}-E_8$ intertwiner shown in Figure 7 are much bigger than those of $A_{17}-E_7$. Moreover, since the element (15,5) of the adjacency matrix is 2, we treat it as two nonzero elements (15,1,5) and (15,2,5) distinguished by a bond variable taking the values 1 or 2. The cell graphs need this extra bond variable to label the two different bonds between the given nodes. If

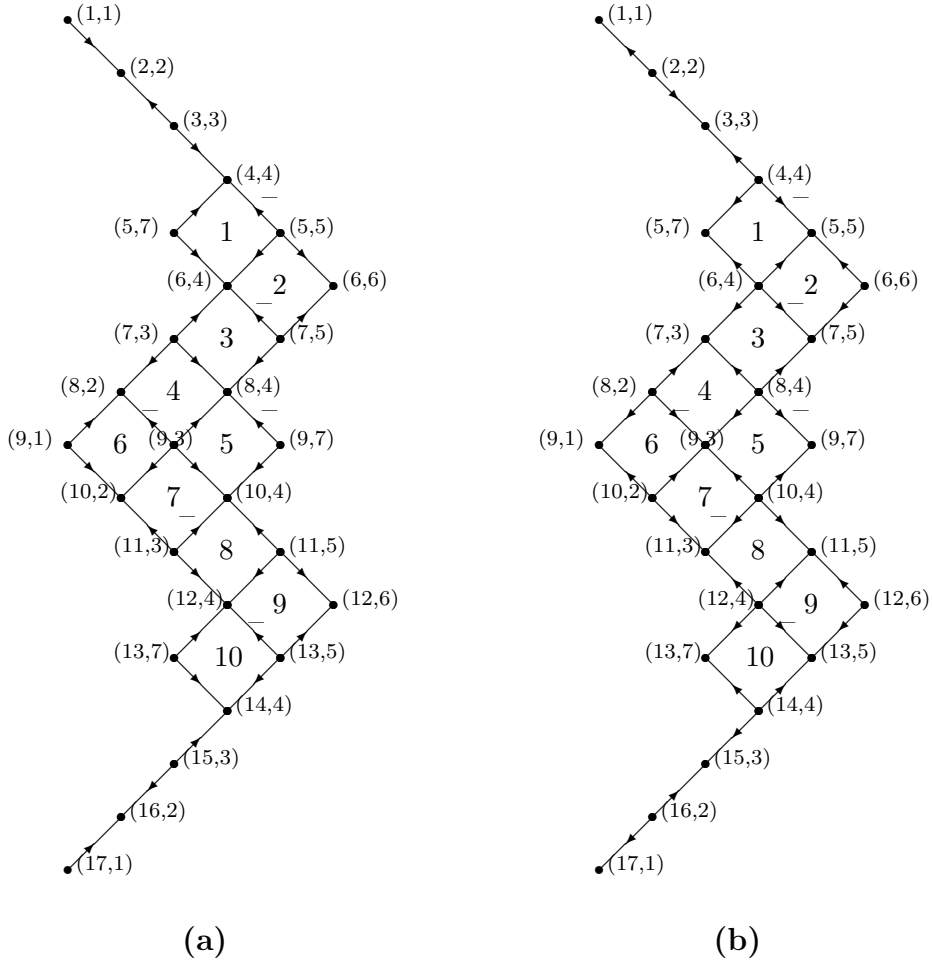


Figure 6. The cell graphs for the $A_{17}-E_7$ intertwiner. The negative signs indicate that the value of the cell associated with that bond is negative, for example, $C(4, 4, 5, 5) = -\cos m_1$.

there is only one bond state we label it by 1. In the cell graphs we mark the negative cells by minus signs in the upper parts of the two graphs. The cells in the lower parts that occur in faces 1 through to 12 are related to the cells in the upper parts by the height reversal symmetry of the A model

$$\begin{array}{ccc}
 & (c, d) & \\
 & \bullet & \\
 (a, b) & \swarrow \quad \searrow & (a, e) \\
 & \bullet & \\
 & (f, d) & \\
 \end{array}
 =
 \begin{array}{ccc}
 & (30 - f, d) & \\
 & \bullet & \\
 (30 - a, b) & \swarrow \quad \searrow & (30 - a, e) \\
 & \bullet & \\
 & (30 - c, d) & \\
 \end{array}
 \quad (3.31)$$

A similar equation holds with the direction of the arrows reversed.

Using the four rules given above we can find all of the cells on the twelve numbered faces. The cells on the faces containing the special elements $(15, 1, 5)$ and $(15, 2, 5)$ have to be studied separately. The parts of the cell graphs around the special elements $(15, 1, 5)$ and $(15, 2, 5)$ are drawn magnified in Figure 8.

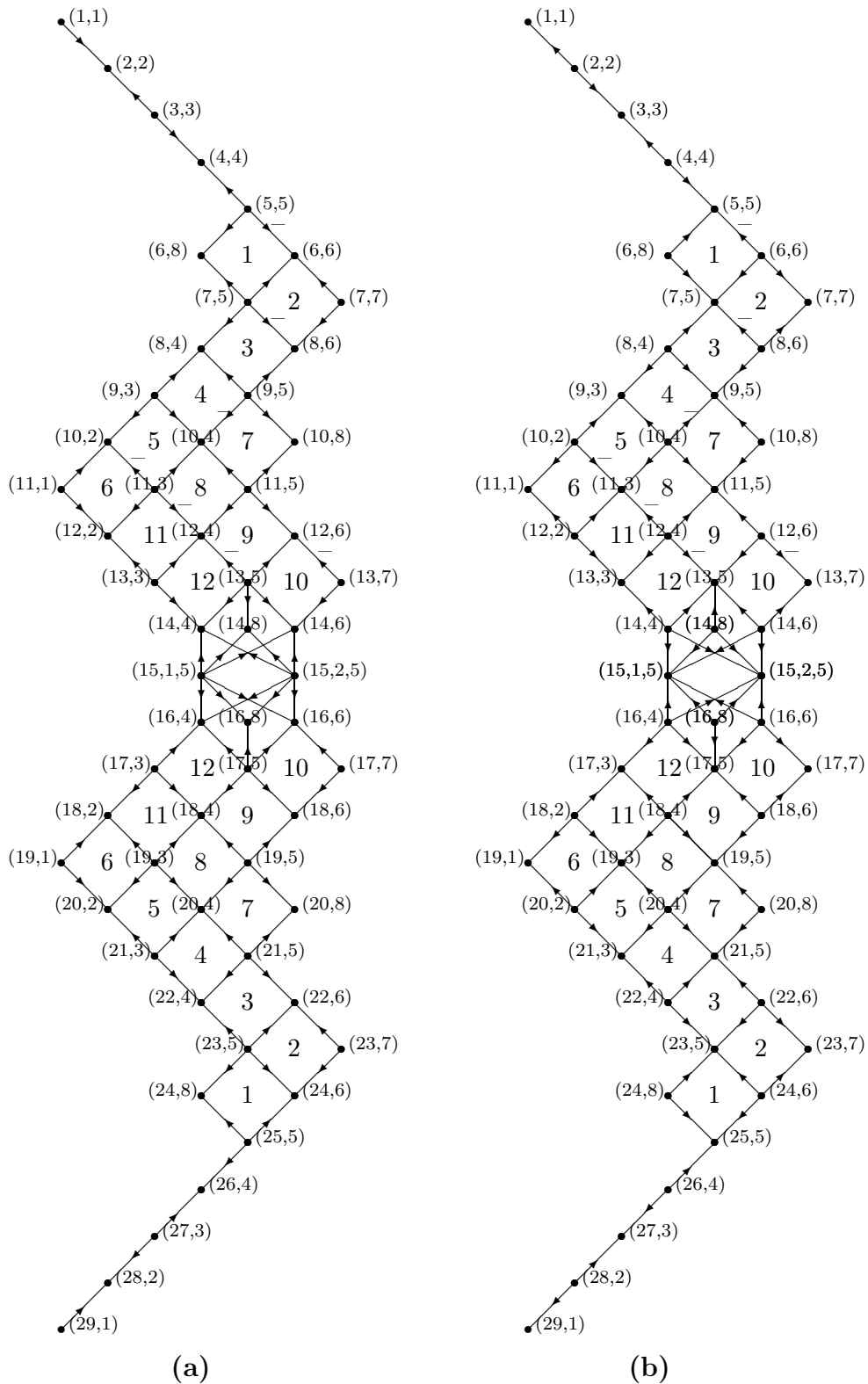


Figure 7. The cell graphs of the $A_{29}-E_8$ intertwiner. The negative cells are indicated with a minus sign in the upper parts of the graphs. The cells in the lower part are related to the cells in the upper part by the height reversal symmetry of the A model.

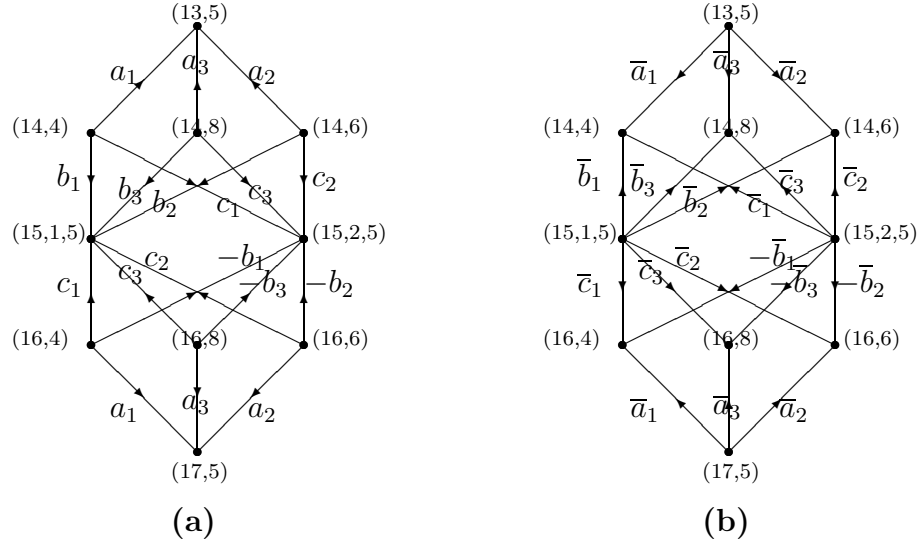


Figure 8. Magnified view of the $A_{29}-E_8$ cell graphs in the vicinity of the special elements $(15, 1, 5)$ and $(15, 2, 5)$ showing the symbols used to denote the values of the cells.

We have used symbols to represent the values of the cells on the bonds in the vicinity of the special elements $(15, 1, 5)$ and $(15, 2, 5)$. The same symbol has been used to denote cells with the same values. Let us define a 3×3 matrix using the cells in the upper part of Figure 8a

$$\begin{pmatrix}
 \begin{array}{ccc}
 \begin{array}{c} 14 \\ \downarrow \\ 13 \\ \downarrow \\ 15 \end{array} & \begin{array}{c} \xrightarrow{1} \\ \downarrow \\ \xrightarrow{1} \end{array} & \begin{array}{c} 8 \\ \downarrow \\ 5 \\ \downarrow \\ 5 \end{array} &
 \begin{array}{ccc}
 \begin{array}{c} 14 \\ \downarrow \\ 13 \\ \downarrow \\ 15 \end{array} & \begin{array}{c} \xrightarrow{1} \\ \downarrow \\ \xrightarrow{1} \end{array} & \begin{array}{c} 6 \\ \downarrow \\ 5 \\ \downarrow \\ 5 \end{array} &
 \begin{array}{ccc}
 \begin{array}{c} 14 \\ \downarrow \\ 13 \\ \downarrow \\ 15 \end{array} & \begin{array}{c} \xrightarrow{1} \\ \downarrow \\ \xrightarrow{1} \end{array} & \begin{array}{c} 4 \\ \downarrow \\ 5 \\ \downarrow \\ 5 \end{array}
 \end{array}
 \end{pmatrix}
 =
 \begin{pmatrix}
 a_3 & a_2 & a_1 \\
 b_3 & b_2 & b_1 \\
 c_3 & c_2 & c_1
 \end{pmatrix}
 \quad (3.32)$$

It is easy to see that these cells satisfy the first unitarity condition if the matrix is orthogonal. Since the matrix can be taken as a coordinate transformation in three dimensional space we can write its elements in terms of the Euler angles α, β, γ

$$\begin{aligned}
 a_1 &= \sin \gamma \\
 a_2 &= \sin \alpha \cos \gamma \\
 a_3 &= \cos \alpha \cos \gamma \\
 b_1 &= \sin \beta \cos \gamma \\
 b_2 &= \cos \alpha \cos \beta - \sin \alpha \sin \gamma \sin \beta \\
 b_3 &= -\sin \alpha \cos \beta - \cos \alpha \sin \gamma \sin \beta
 \end{aligned}
 \quad (3.33)$$

$$\begin{aligned}
c_1 &= \cos \beta \cos \gamma \\
c_2 &= -\cos \alpha \sin \beta - \sin \alpha \sin \gamma \cos \beta \\
c_3 &= \sin \alpha \sin \beta - \cos \alpha \sin \gamma \cos \beta.
\end{aligned}$$

The Euler angles can be determined from the second unitarity condition. Consider the three quadrilateral faces formed by the elements $(14, 2i)$, $(16, 2i)$, $(15, 1, 5)$ and $(15, 2, 5)$ in Figure 8a where $i = 2, 3, 4$. The cells on these faces should satisfy three sets of equations required by the second unitarity condition. Setting

$$\begin{aligned}
C \begin{pmatrix} 16 & 2i \\ 15 & 1 & 5 \end{pmatrix} &= c_{i-1}, \quad i = 2, 3, 4 \\
C \begin{pmatrix} 16 & 2i \\ 15 & 2 & 5 \end{pmatrix} &= -b_{i-1}, \quad i = 2, 3, 4
\end{aligned} \tag{3.34}$$

these three sets of equations read

$$b_i^2 + c_i^2 = S_{15}^A S_{2i}^E / (S_{14}^A S_5^E), \quad i = 2, 3, 4. \tag{3.35}$$

Substituting b and c into the above equations, we have

$$\cos \gamma = \sqrt{S_{15}^A S_4^E / (S_{14}^A S_5^E)} \quad \text{for } i = 2 \tag{3.36}$$

$$\sin \alpha = \sqrt{\frac{S_{14}^A S_5^E - S_{15}^A S_6^E}{S_{15}^A S_4^E}} \quad \text{for } i = 3 \text{ or } 4 \tag{3.37}$$

The variable β is not determined by the above equations and we simply take $\beta = \alpha$. It is easy to check that taking

$$C \begin{pmatrix} 16 & 2i \\ 17 & 5 \end{pmatrix} = a_{i-1} \quad i = 2, 3, 4 \tag{3.38}$$

satisfies the unitarity conditions.

In Figure 8b the nine cells with values in the matrix

$$\begin{pmatrix} \bar{a}_3 & \bar{a}_2 & \bar{a}_1 \\ \bar{b}_3 & \bar{b}_2 & \bar{b}_1 \\ \bar{c}_3 & \bar{c}_2 & \bar{c}_1 \end{pmatrix}$$

are required to satisfy the second unitarity condition. We easily see that the second unitarity condition is obtainable from the first unitarity condition with

$$\begin{aligned}
\bar{a}_i &= a_i \sqrt{S_{14}^A S_5^E / (S_{13}^A S_{2i+2}^E)} \quad i = 1, 2, 3 \\
\bar{b}_i &= b_i \sqrt{S_{14}^A S_5^E / (S_{15}^A S_{2i+2}^E)} \quad i = 1, 2, 3 \\
\bar{c}_i &= c_i \sqrt{S_{14}^A S_5^E / (S_{15}^A S_{2i+2}^E)} \quad i = 1, 2, 3
\end{aligned} \tag{3.39}$$

The cells on the three faces formed by the elements $(14, 2i)$, $(16, 2i)$, $(15, 1, 5)$ and $(15, 2, 5)$ in Figure 8b should satisfy the first unitarity condition. So we can simply take

$$C \begin{pmatrix} 15 & 1 & 5 \\ 16 & & 2i \end{pmatrix} = \bar{c}_{i-1}, \quad C \begin{pmatrix} 15 & 2 & 5 \\ 16 & & 2i \end{pmatrix} = -\bar{b}_{i-1} \tag{3.40}$$

and

$$C \begin{pmatrix} 17 & 5 \\ 16 & 2i \end{pmatrix} = \bar{a}_{i-1}, \quad i = 2, 3, 4 \quad (3.41)$$

On the other hand, the cells $C(14, 4, 5, 13)$ and $C(14, 6, 5, 13)$ occur on the shared bonds of the faces 10 and 12. So of course we can obtain the values \bar{a}_1 and \bar{a}_2 respectively from the faces 12 and 10 using the usual rules. This gives the same results. The complete list of cells for the $A_{29}-E_8$ intertwiner are given in Appendix C4.

This concludes the derivation of the cells for the classical $A-D-E$ intertwiners. All of the cells can be found in Appendix C. They satisfy the two unitarity conditions and the cell intertwining relations.

3.4 Affine $A-D-E$

In this section we obtain the intertwining cells for the affine $A-D-E$ models. We first draw the cell graphs and find the absolute values of the cells using our previous four rules or, equivalently, the unitarity relations. To determine the remaining signs we use the intertwining relation of the affine models.

The adjacency matrix C for the affine $A_{L-1}^{(1)}-D_{\frac{L}{2}+2}^{(1)}$ intertwiner is given in Appendix B. Note that the spins L and 1 are neighbours for the affine A model. We obtain the cell graph shown in Figure 9 for the affine $A_{L-1}^{(1)}-D_{\frac{L}{2}+2}^{(1)}$ model. The values of the cells can be obtained as before. The negative signs in the the cell graphs indicate the cells that are negative. Therefore we can read off the values of all the cells from the cell graphs. It is easily verified that these cells intertwine the faces of the affine $A-D$ models even for arbitrary crossing parameter λ . The results for the cells are listed in Appendix D1.

The adjacency matrices C for the $A_5^{(1)}-E_6^{(1)}$, $A_7^{(1)}-E_7^{(1)}$ and $A_9^{(1)}-E_8^{(1)}$ intertwiners are also given in Appendix B. The cell graphs for these intertwiners are shown in Figures 10–12 respectively. We have indicated which cells are negative in the graphs. We obtain all of the cells for the $A_5^{(1)}-E_6^{(1)}$ and $A_7^{(1)}-E_7^{(1)}$ intertwiners by applying our previous rules. For the $A_9^{(1)}-E_8^{(1)}$ intertwiner we need to treat the doubly degenerate element (6, 6) by introducing bond variables as we did for the classical $A_{29}-E_8$ intertwiner. The cell graphs of the $A_9^{(1)}-E_8^{(1)}$ intertwiner contains three parts: the upper part containing the faces 1–9, the middle part around the elements (6, 1, 6) and (6, 2, 6) and the lower part containing the faces 1–6. By our rules the absolute values of the cells in the upper part are the same as those in the lower part, that is, $|C(a, 1, b, c, 1, d)| = |C(12 - a, 1, b, c, 1, 12 - d)|$. So we have marked the faces in the lower part by the same number as the symmetric faces in the upper part. However, the intertwining relation of the models does not give the same sign for $C(a, 1, b, c, 1, d)$ and $C(12 - a, 1, b, c, 1, 12 - d)$ generally. We can treat the middle part in the same way as the $A_{29}-E_8$ case. The cell graphs for this part are shown magnified in Figure 13.

Following the arguments for the $A_{29}-E_8$ intertwiner we obtain the following results

$$b_i^2 + c_i^2 = \sqrt{\frac{S_{3+2i}^E}{S_6^E}} \quad i = 1, 2, 3. \quad (3.42)$$

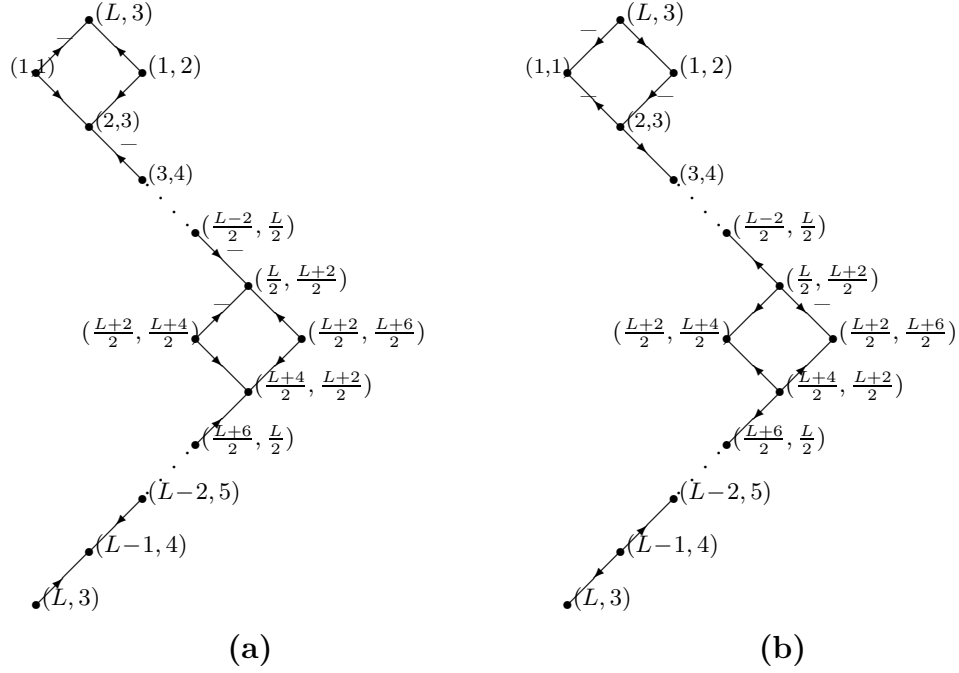


Figure 9. The cell graphs of the $A_{L-1}^{(1)} - D_{\frac{L}{2}+2}^{(1)}$ intertwiner. The negative signs indicate that the cell associated with that bond is negative.

Substituting b and c into the above equations, we have

$$\cos \gamma = \sqrt{\frac{S_5^E}{S_6^E}} \quad \text{for } i = 1; \quad (3.43)$$

$$\sin \alpha = \sqrt{\frac{S_6^E - S_7^E}{S_5^E}} \quad \text{for } i = 2 \text{ or } 3. \quad (3.44)$$

We simply set $\beta = \alpha$. We also find

$$\bar{a}_i = a_i \sqrt{\frac{S_6^E}{S_{2i+3}^E}} \quad i = 1, 2, 3; \quad (3.45)$$

$$\bar{b}_i = b_i \sqrt{\frac{S_6^E}{S_{2i+3}^E}} \quad i = 1, 2, 3; \quad (3.46)$$

$$\bar{c}_i = c_i \sqrt{\frac{S_6^E}{S_{2i+3}^E}} \quad i = 1, 2, 3. \quad (3.47)$$

In this way we obtain all the cells for the affine A - D and A - E intertwiners. These cells satisfy the unitarity conditions and the intertwining relations. We list all of the cells for the affine A - D - E intertwiners in Appendix D.

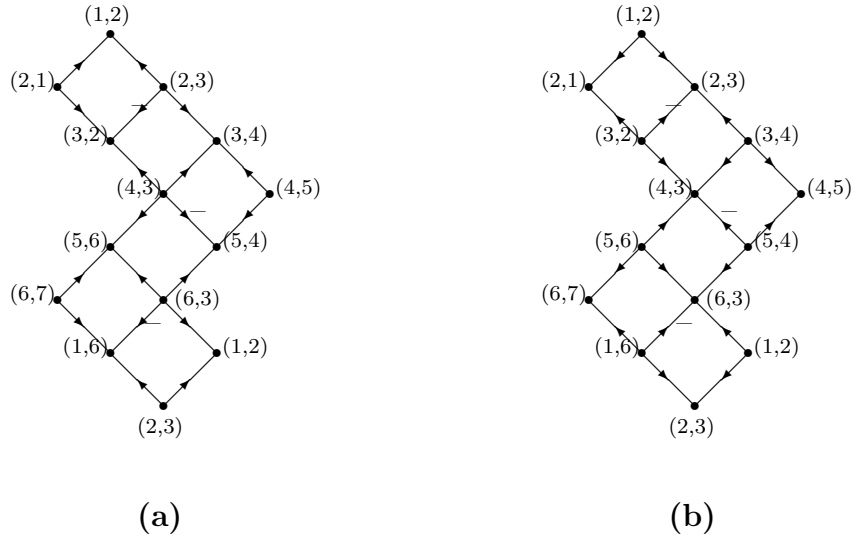


Figure 10. The cell graphs of the $A_5^{(1)}-E_6^{(1)}$ intertwiner. The negative signs indicate that the cell associated with that bond is negative.

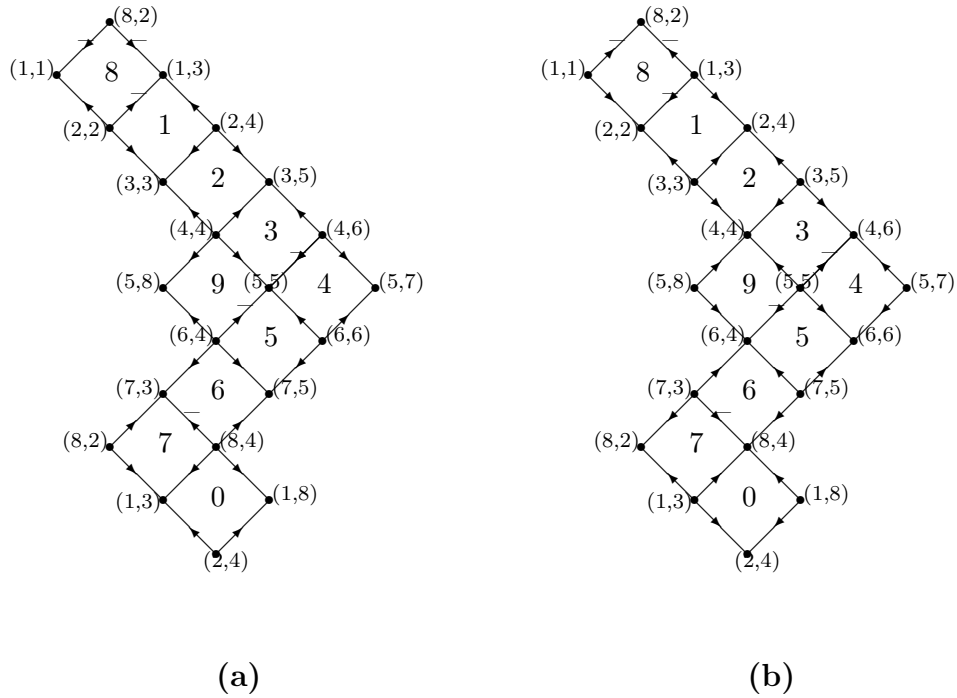


Figure 11. The cell graphs of the $A_7^{(1)}-E_7^{(1)}$ intertwiner. The negative signs indicate that the cell associated with that bond is negative.

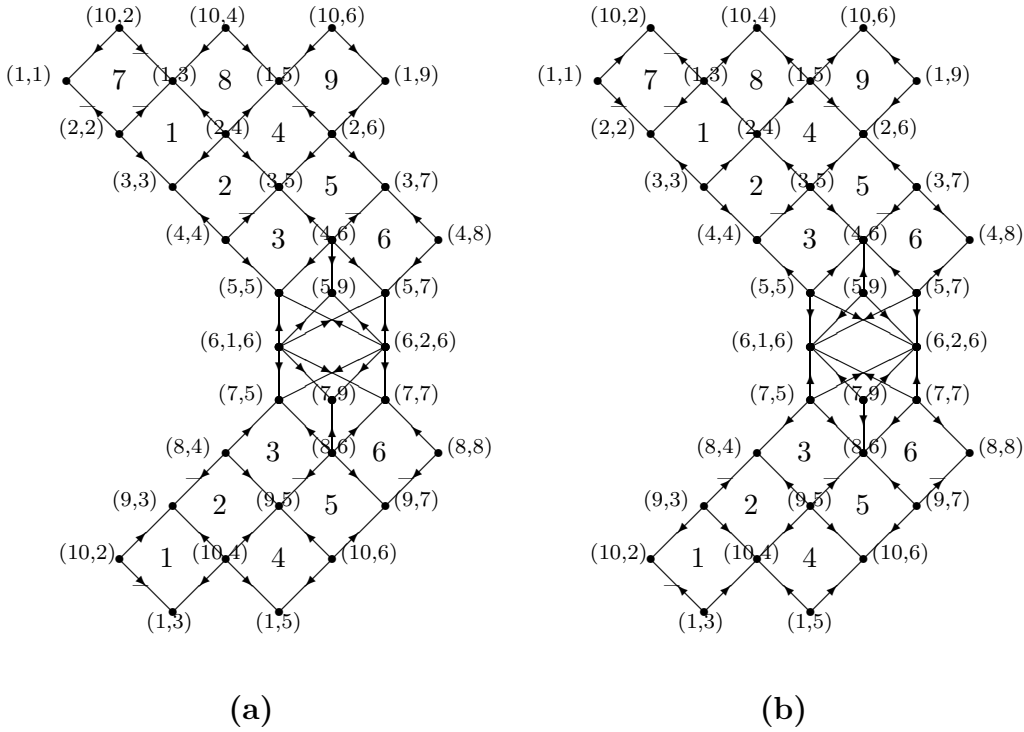


Figure 12. The cell graphs of the $A_9^{(1)}-E_8^{(1)}$ intertwiner. The negative signs indicate that the cell associated with that bond is negative.

3.5 Dilute $A-D-E$

In this section consider the intertwining cells for the critical classical dilute $A-D-E$ models. We use rules 1–4 and the cell graphs of the usual $A-D-E$ models to obtain the cells for the dilute models. The nonzero cells of the classical dilute $A-D-E$ models are exactly the same as those for the corresponding classical Temperley-Lieb $A-D-E$ models except that there are extra nonzero cells for the dilute models. The number of the extra cells is just the sum of the nonzero elements of the adjacency matrix of the adjacency intertwiner. For example, we find 15 extra nonzero cells for the dilute $A_{11}-E_6$ intertwiner and 58 extra nonzero cells for the dilute $A_{29}-E_8$. These extra cells all occur on the nodes (nonzero elements of the adjacency matrix of the intertwiner) and all take the value 1 or -1 . This means that the extra nonzero cells are given by

$$C \begin{pmatrix} a & b \\ a & b \end{pmatrix} = 1; \text{ if the element } (a, b) \text{ of the adjacency matrix } C \text{ is } 1$$

for the dilute $A-D$, $A_{11}-E_6$ and $A_{17}-E_7$ models and by

$$C \begin{pmatrix} a & s & b \\ a & s & b \end{pmatrix} = (-1)^{(s-1)}; \text{ if the element } (a, b) \text{ of the adjacency matrix } C \text{ is } 1$$

for the dilute $A_{29}-E_8$ models where the bond variable $s = 1, 2$. These cells satisfy the unitarity conditions and the intertwining relations.

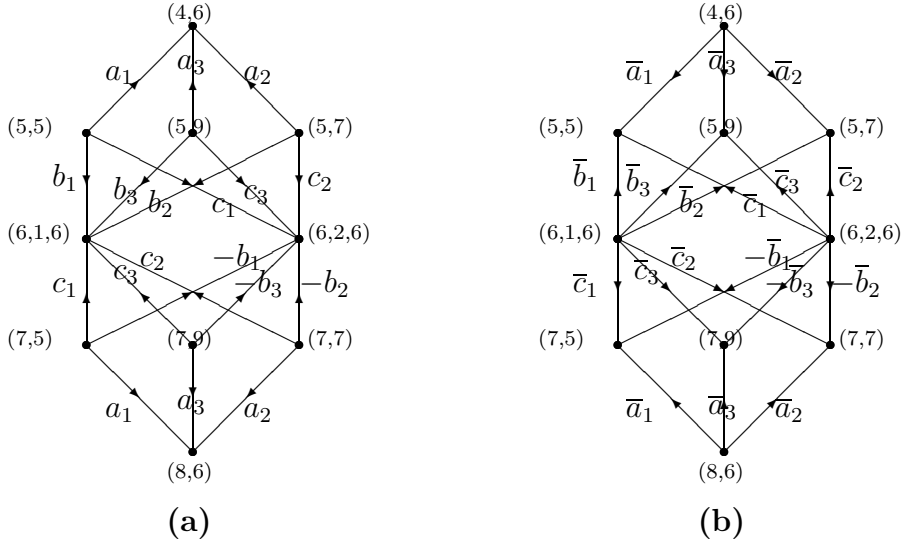


Figure 13. Magnified view of the $A_9^{(1)}-E_8^{(1)}$ cell graphs in the vicinity of the special elements $(6, 1, 6)$ and $(6, 2, 6)$.

4 Row Transfer Matrix Intertwiners

In this section we study intertwiners relating the row transfer matrices of $A-D-E$ models. This is the third level of the intertwining relation. The first two levels relate the adjacency matrices and the face weights. These three levels are closely related. Suppose that \mathbf{a} and \mathbf{b} are allowed spin configurations of two consecutive rows of N (even) spins with periodic boundary conditions. The elements of the row transfer matrix $\mathbf{T}(u)$ are given by

$$\begin{aligned}
 \langle \mathbf{a} | \mathbf{T}(u) | \mathbf{b} \rangle &= \prod_{j=1}^N W \left(\begin{array}{cc|c} b_j & b_{j+1} & u \\ a_j & a_{j+1} & \end{array} \right) \\
 &= \begin{array}{c} \begin{array}{cccccccc} b_1 & b_2 & & & & & & b_{N+1} \\ \hline \begin{array}{cccccccc} \leftarrow & \leftarrow & \leftarrow & \leftarrow & \leftarrow & \leftarrow & \leftarrow & \leftarrow \\ \hline \begin{array}{cccccccc} a_1 & a_2 & & & & & & a_{N+1} \end{array} \end{array} \end{array} \end{array} \quad (4.1)
 \end{aligned}$$

where $a_{N+1} = a_1$ and $b_{N+1} = b_1$. The Yang-Baxter equation implies the commutation relations

$$[\mathbf{T}(u), \mathbf{T}(v)] = 0. \quad (4.2)$$

More precisely, the proof [12] uses the Yang-Baxter equation and unitarity.

Let us consider the row transfer matrices in the braid limits and define

$$\mathcal{B}, \bar{\mathcal{B}} = \lim_{u \rightarrow \mp i\infty} \left(\frac{\sin \lambda}{\sin(u - \lambda/2)} \right)^N \mathbf{T}(u) \quad (4.3)$$

then clearly

$$[\mathbf{T}(u), \mathcal{B}] = [\mathbf{T}(u), \bar{\mathcal{B}}] = 0 \quad (4.4)$$

so that \mathcal{B} and $\overline{\mathcal{B}}$ can be simultaneously diagonalized with $\mathbf{T}(u)$. Moreover, in this braid limit, it can be shown [21] that the eigenvalues of \mathcal{B} and $\overline{\mathcal{B}}$ are given by

$$2 \cos m_j, \quad 2 \cos \overline{m}_j \quad (4.5)$$

where m_j and \overline{m}_j are the Coxeter exponents of the relevant A - D - E model. In this way, the Coxeter exponents (m_j, \overline{m}_j) are seen as quantum numbers labelling the sectors of row transfer matrix eigenvalues. It can also be shown [20] that for the row transfer matrices of the A_L models $\mathcal{B}_A = \overline{\mathcal{B}}_A$ and hence $m_j = \overline{m}_j$. The braid row transfer matrices play a similar role at the row transfer matrix level to the role played by the adjacency matrices at the level of the adjacency matrices.

Let us denote the row transfer matrices of two A - D - E models by \mathcal{A} and \mathcal{G} . Invariably, if an intertwiner exists, the largest eigenvalue of these matrices is in common. Since this eigenvalue is exactly the same for a finite size system, the corresponding critical models will have the same finite size corrections and hence the same central charge c in the thermodynamic limit. For the affine A - D - E models this is $c = 1$. For the classical A - D - E models the central charge is

$$c = 1 - \frac{6}{h(h-1)} \quad (4.6)$$

and, similarly, the conformal weights

$$(\Delta_{r,s}, \overline{\Delta}_{r,s}) \quad (4.7)$$

of the excited states corresponding to the other common eigenvalues will be exactly the same [20, 21] where r and s label the columns and rows of the Kac table. Indeed, in this case, it turns out [20] that the row label s in the Kac Table is given precisely by the Coxeter exponents

$$s = m_j. \quad (4.8)$$

4.1 Construction of Row Intertwiners

We construct the intertwiners between A - D - E row transfer matrices from the cells obtained in Section 3. Let \mathcal{A} and \mathcal{G} be row transfer matrices of two A - D - E models. Using the intertwining relation (3.12) for the face weights and the unitarity conditions for the cells we can easily construct the intertwiner for the row transfer matrices \mathcal{A} and \mathcal{G} . The intertwining relation

$$\mathcal{A}(u)\mathcal{C} = \mathcal{C}\mathcal{G}(u) \quad (4.9)$$

can be pictured as follows

$$\begin{array}{c}
 \begin{array}{c}
 \begin{array}{ccccccccccc}
 a'_1 & a'_2 & & & & & & & & & a'_{N+1} = a'_1 \\
 \downarrow & \downarrow & \downarrow & \downarrow & \downarrow & \downarrow & \downarrow & \downarrow & \downarrow & \downarrow & \downarrow \\
 b & & & & & & & & & & b \\
 \downarrow & \downarrow & \downarrow & \downarrow & \downarrow & \downarrow & \downarrow & \downarrow & \downarrow & \downarrow & \downarrow \\
 a_1 & a_2 & & & & & & & & & a_{N+1} = a_1 \\
 \end{array} \\
 \mathcal{C} \\
 \mathcal{A} \\
 \end{array} \\
 = \\
 \begin{array}{c}
 \begin{array}{ccccccccccc}
 a'_1 & a'_2 & & & & & & & & & a'_{N+1} = a'_1 \\
 \downarrow & \downarrow & \downarrow & \downarrow & \downarrow & \downarrow & \downarrow & \downarrow & \downarrow & \downarrow & \downarrow \\
 b & & & & & & & & & & b \\
 \downarrow & \downarrow & \downarrow & \downarrow & \downarrow & \downarrow & \downarrow & \downarrow & \downarrow & \downarrow & \downarrow \\
 a_1 & a_2 & & & & & & & & & a_{N+1} = a_1 \\
 \end{array} \\
 \mathcal{G} \\
 \mathcal{C} \\
 \end{array}
 \end{array} \quad (4.10)$$

where the solid circles mean summation over the corresponding spins. The row intertwiner \mathcal{C} is constructed from N cells with periodic boundary conditions. Specifically, if \mathbf{a} and \mathbf{b} are allowed row configurations of the graph A and G with periodic boundary conditions $a_{N+1} = a_1$ and $b_{N+1} = b_1$, then the elements of the row intertwiner are given by

$$\langle \mathbf{a} | \mathcal{C} | \mathbf{b} \rangle = \begin{array}{c} \begin{array}{cccccccccccc} & b_1 & & b_2 & & & & & & & & & & b_{N+1} \\ \leftarrow & \leftarrow & \leftarrow & \leftarrow & \leftarrow & \leftarrow & \leftarrow & \leftarrow & \leftarrow & \leftarrow & \leftarrow & \leftarrow & \leftarrow & \leftarrow \\ \leftarrow & \leftarrow & \leftarrow & \leftarrow & \leftarrow & \leftarrow & \leftarrow & \leftarrow & \leftarrow & \leftarrow & \leftarrow & \leftarrow & \leftarrow & \leftarrow \\ & a_1 & & a_2 & & & & & & & & & & a_{N+1} \end{array} \\ \end{array} \quad (4.11)$$

Generally, the row intertwiner is a rectangular matrix. The proof of the intertwining relation (4.10) between the row transfer matrices proceeds in exactly the same way as the proof of the commutation relation (4.2) with the cell intertwiner relation playing the role of the Yang-Baxter relation.

4.2 Properties of Row Intertwiners

The intertwining relation between row transfer matrices is an equivalence relation even though the row transfer matrices are not in general symmetric. The symmetry of the relation follows from the crossing symmetry

$$\mathcal{G}(u)^T = \mathcal{G}(\lambda - u). \quad (4.12)$$

The row intertwiner projects the eigenvectors of the transfer matrix \mathcal{A} corresponding to common eigenvalues onto those of \mathcal{G} and annihilates all eigenvectors corresponding to eigenvalues which are not in common.

Let us consider the symmetry operators given by the square matrices $\mathcal{C}\mathcal{C}^T$ and $\mathcal{C}^T\mathcal{C}$. Just as for the adjacency matrix level, we can show that

$$[\mathcal{C}\mathcal{C}^T, \mathcal{A}(u)] = [\mathcal{C}^T\mathcal{C}, \mathcal{G}(u)] = 0 \quad (4.13)$$

so that the row transfer matrix and its corresponding symmetry operator have the same eigenvectors and can be simultaneously diagonalized. The eigenvectors that are not annihilated by the symmetry operators give the eigenvalues that are intertwined or common to \mathcal{A} and \mathcal{G} . Moreover,

$$\mathcal{C}\mathcal{C}^T \stackrel{\mathcal{C}}{\sim} \mathcal{C}^T\mathcal{C} \quad (4.14)$$

so that the nonzero eigenvalues of these symmetry operators are in common.

4.3 An Example: The A - D Row Intertwiner

Let us now consider the A_L - $D_{(L+3)/2}$ models and define the height reversal operators \mathcal{R}_A and \mathcal{R}_D for the A and D models by the elements

$$\langle \mathbf{a} | \mathcal{R}_A | \mathbf{b} \rangle = \prod_{j=1}^N \delta_{a_j, r(b_j)}, \quad \langle \mathbf{a} | \mathcal{R}_D | \mathbf{b} \rangle = \prod_{j=1}^N \delta_{a_j, r(b_j)} \quad (4.15)$$

where for the A model $r(b) = h - b$ and for the D model $r(b) = b$ for $b = 1, 2, \dots, (L-1)/2$, $r((L+1)/2) = (L+3)/2$ and $r((L+3)/2) = (L+1)/2$. These matrix operators reflect the \mathbb{Z}_2 symmetry of the models. We show that

$$\mathcal{C}\mathcal{C}^T = I + \mathcal{R}_A, \quad \mathcal{C}^T\mathcal{C} = I + \mathcal{R}_D \quad (4.16)$$

An immediate consequence of this is that the eigenvalues of \mathcal{A} and \mathcal{D} are in common if and only if the corresponding eigenvectors are even under the \mathbb{Z}_2 symmetry. In particular, since the largest eigenvalue has an even eigenvector, the largest eigenvalue is in common.

The proof of (4.16) is straightforward. Using the adjacency conditions of the graphs A_L and $D_{(L+3)/2}$, we easily see that the operators $\mathcal{C}\mathcal{C}^T$ or $\mathcal{C}^T\mathcal{C}$ can be decomposed into two nonzero terms pictured as follows

$$\begin{aligned} \langle \mathbf{a} | \mathcal{C}\mathcal{C}^T | \mathbf{b} \rangle &= \begin{array}{c} \begin{array}{cccccccc} b_1 & b_2 & & & & & & b_{N+1} = b_1 \\ \hline \begin{array}{cccccccc} \leftarrow & \leftarrow & \leftarrow & \leftarrow & \leftarrow & \leftarrow & \leftarrow & \leftarrow \\ \hline \begin{array}{cccccccc} c & & & & & & & c \\ \hline \begin{array}{cccccccc} \leftarrow & \leftarrow & \leftarrow & \leftarrow & \leftarrow & \leftarrow & \leftarrow & \leftarrow \\ \hline \begin{array}{cccccccc} a_1 & a_2 & & & & & & a_{N+1} = a_1 \end{array} \end{array} \end{array} \end{array} \\ &= \begin{array}{c} \begin{array}{cccccccc} a_1 & a_2 & & & & & & a_{N+1} = a_1 \\ \hline \begin{array}{cccccccc} \leftarrow & \leftarrow & \leftarrow & \leftarrow & \leftarrow & \leftarrow & \leftarrow & \leftarrow \\ \hline \begin{array}{cccccccc} c & & & & & & & c \\ \hline \begin{array}{cccccccc} \leftarrow & \leftarrow & \leftarrow & \leftarrow & \leftarrow & \leftarrow & \leftarrow & \leftarrow \\ \hline \begin{array}{cccccccc} a_1 & a_2 & & & & & & a_{N+1} = a_1 \end{array} \end{array} \end{array} \end{array} \prod_{j=1}^N \delta_{a_j, b_j} \\ &+ \begin{array}{c} \begin{array}{cccccccc} r(a_1) & r(a_2) & & & & & & r(a_{N+1}) = r(a_1) \\ \hline \begin{array}{cccccccc} \leftarrow & \leftarrow & \leftarrow & \leftarrow & \leftarrow & \leftarrow & \leftarrow & \leftarrow \\ \hline \begin{array}{cccccccc} c & & & & & & & c \\ \hline \begin{array}{cccccccc} \leftarrow & \leftarrow & \leftarrow & \leftarrow & \leftarrow & \leftarrow & \leftarrow & \leftarrow \\ \hline \begin{array}{cccccccc} a_1 & a_2 & & & & & & a_{N+1} = a_1 \end{array} \end{array} \end{array} \end{array} \prod_{j=1}^N \delta_{r(a_j), b_j} \end{array} \end{array} \quad (4.17)$$

A similar picture can be drawn for $\langle \mathbf{a} | \mathcal{C}^T\mathcal{C} | \mathbf{b} \rangle$. The solid circles indicate summation. Since the A and D models possess \mathbb{Z}_2 symmetry, the row transfer matrices of the models commute with the corresponding height reversal operators.

It is relatively simple to determine if an eigenvector is even or odd under the given \mathbb{Z}_2 symmetry. Indeed, for the row transfer matrix \mathcal{A} , the quantum number under the \mathbb{Z}_2 symmetry

$$\mathcal{R}_A = \mathcal{U}^{(L-1)}(\mathcal{B}_A) \quad (4.18)$$

is given by

$$r_A = \mathcal{U}^{(L-1)}(2 \cos m_j) = \begin{cases} 1, & m_j \text{ odd} \\ -1, & m_j \text{ even} \end{cases} \quad (4.19)$$

where $2 \cos m_j$ is the corresponding eigenvalue of the braid transfer matrix $\mathcal{B}_A = \overline{\mathcal{B}}_A$. For the A - D models we therefore conclude that the overlap of the row transfer matrix eigenvalues is as shown pictorially in Figure 14.

This overlap can be interpreted in the thermodynamic limit in terms of conformal weights, or better, in terms of modular invariant partition functions. Let us consider the A_5 - D_4 intertwiner relating the tetracritical Ising model to the critical 3-state Potts model in the ferromagnetic regime $u > 0$. The conformal weights in this case are shown

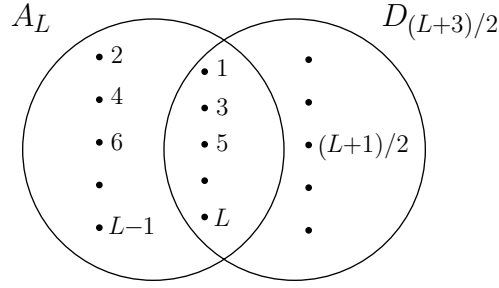


Figure 14. Pictorial representation of the overlap of the A_L and $D_{(L+3)/2}$ row transfer matrix eigenvalues. The common eigenvalues have quantum numbers given by the Coxeter exponents $m_j = \bar{m}_j = 1, 3, 5, \dots, L$ and are even under the \mathbb{Z}_2 symmetry. The other eigenvalues are odd under the \mathbb{Z}_2 symmetry. The eigenvalues lying in A but not in D have quantum numbers $m_j = \bar{m}_j = 2, 4, 6, \dots, L - 1$ whereas the eigenvalues lying in D but not A have quantum numbers $\bar{m}_j = L + 1 - m_j$ so that $m_j \neq \bar{m}_j$ except for $m_j = \bar{m}_j = (L + 1)/2$.

$s = m_j$					
5	3	7/5	2/5	0	
4	13/8	21/40	1/40	1/8	
3	2/3	1/15	1/15	2/3	
2	1/8	1/40	21/40	13/8	
1	0	2/5	7/5	3	
	1	2	3	4	r

Table 3. Grid of conformal weights $\Delta_{r,s}$ for $h = 6$. The row index s is identified with the Coxeter exponent m_j . Only the left half of the table with $r = 1, 2$ is needed.

in Table 3. We find that the towers of eigenvalues in the two modular invariant partition functions are divided as follows:

$$\begin{aligned}
 \text{In } A_5 \text{ and } D_4: & \quad |\chi_0|^2 + |\chi_3|^2 + |\chi_{2/5}|^2 + |\chi_{7/5}|^2 + |\chi_{1/15}|^2 + |\chi_{2/3}|^2 \\
 \text{In } A_5 \text{ not } D_4: & \quad |\chi_{1/8}|^2 + |\chi_{1/40}|^2 + |\chi_{12/40}|^2 + |\chi_{13/8}|^2 \\
 \text{In } D_4 \text{ not } A_5: & \quad |\chi_{1/15}|^2 + |\chi_{2/3}|^2 + \chi_0 \bar{\chi}_3 + \bar{\chi}_0 \chi_3 + \chi_{2/5} \bar{\chi}_{7/5} + \bar{\chi}_{2/5} \chi_{7/5}.
 \end{aligned} \tag{4.20}$$

Here $\chi_\Delta(q)$ are the Virasoro characters, q is the modular parameter and the bars denote complex conjugation.

A similar picture emerges in the antiferromagnetic regime $u < 0$, at least in the Hamiltonian limit $u \rightarrow 0^-$. This amounts to looking at the other end of the same spectrum as $N \rightarrow \infty$. In this case we find that the towers of eigenvalues in the two modular invariant partition functions are divided as follows:

$$\text{In } A_5 \text{ and } D_4: \quad |b_0^0|^2 + |b_0^2|^2 + |b_0^4|^2 + |b_2^2|^2 + 2|b_2^4|^2$$

$$\begin{aligned}
\text{In } A_5 \text{ not } D_4: & \quad 2|b_1^1|^2 + 2|b_1^3|^2 & (4.21) \\
\text{In } D_4 \text{ not } A_5: & \quad |b_0^2|^2 + |b_2^2|^2 + 2|b_2^4|^2 + b_0^0 \bar{b}_0^4 + \bar{b}_0^0 b_0^4
\end{aligned}$$

where b_m^ℓ are \mathbb{Z}_4 string functions [23]. In this case it is not so easy to relate the values of the quantum number m_j to the indices ℓ and m . A detailed discussion of the spectrum in this case is given by Kedem and McCoy [24] in these proceedings.

5 Conclusion

In this article we have further developed the notion of intertwiners between A - D - E models. Although we have concentrated on the critical cases, the classical and affine A - D intertwiners extend unchanged to the elliptic off-critical models. The intertwiners discussed here can also be extended to the fusion A - D - E models. This will be discussed in a future paper [25].

Acknowledgements

This research has been supported by the Australian Research Council. PAP thanks Prof. Jean Marie Maillard for the invitation to speak in Paris and for the kind hospitality extended to him. The authors also thank David O'Brien for discussions.

A Appendix A: Classical Adjacency Intertwiners

The adjacency matrix intertwiners C for the classical A - D - E models are as follows:

$$\begin{array}{cc}
 \begin{array}{c} A_L-D_{\frac{L+3}{2}} \\ \\ C = \begin{pmatrix} 1 & 0 & \dots & 0 & 0 & 0 \\ 0 & 1 & \dots & 0 & 0 & 0 \\ \vdots & \vdots & \ddots & \vdots & \vdots & \vdots \\ 0 & 0 & \dots & 1 & 0 & 0 \\ 0 & 0 & \dots & 0 & 1 & 1 \\ 0 & 0 & \dots & 1 & 0 & 0 \\ \vdots & \vdots & \ddots & \vdots & \vdots & \vdots \\ 0 & 1 & \dots & 0 & 0 & 0 \\ 1 & 0 & \dots & 0 & 0 & 0 \end{pmatrix} \end{array} &
 \begin{array}{c} A_{11}-E_6 \\ \\ C = \begin{pmatrix} 1 & 0 & 0 & 0 & 0 & 0 \\ 0 & 1 & 0 & 0 & 0 & 0 \\ 0 & 0 & 1 & 0 & 0 & 0 \\ 0 & 0 & 0 & 1 & 0 & 1 \\ 0 & 0 & 1 & 0 & 1 & 0 \\ 0 & 1 & 0 & 1 & 0 & 0 \\ 1 & 0 & 1 & 0 & 0 & 0 \\ 0 & 1 & 0 & 0 & 0 & 1 \\ 0 & 0 & 1 & 0 & 0 & 0 \\ 0 & 0 & 0 & 1 & 0 & 0 \\ 0 & 0 & 0 & 0 & 1 & 0 \end{pmatrix} \end{array} \\
 \\
 \begin{array}{c} A_{17}-E_7 \\ \\ C = \begin{pmatrix} 1 & 0 & 0 & 0 & 0 & 0 & 0 \\ 0 & 1 & 0 & 0 & 0 & 0 & 0 \\ 0 & 0 & 1 & 0 & 0 & 0 & 0 \\ 0 & 0 & 0 & 1 & 0 & 0 & 0 \\ 0 & 0 & 0 & 0 & 1 & 0 & 1 \\ 0 & 0 & 0 & 1 & 0 & 1 & 0 \\ 0 & 0 & 1 & 0 & 1 & 0 & 0 \\ 0 & 1 & 0 & 1 & 0 & 0 & 0 \\ 1 & 0 & 1 & 0 & 0 & 0 & 1 \\ 0 & 1 & 0 & 1 & 0 & 0 & 0 \\ 0 & 0 & 1 & 0 & 1 & 0 & 0 \\ 0 & 0 & 0 & 1 & 0 & 1 & 0 \\ 0 & 0 & 0 & 0 & 1 & 0 & 1 \\ 0 & 0 & 0 & 1 & 0 & 0 & 0 \\ 0 & 0 & 1 & 0 & 0 & 0 & 0 \\ 0 & 1 & 0 & 0 & 0 & 0 & 0 \\ 1 & 0 & 0 & 0 & 0 & 0 & 0 \end{pmatrix} \end{array} &
 \begin{array}{c} A_{29}-E_8 \\ \\ C = \begin{pmatrix} 1 & 0 & 0 & 0 & 0 & 0 & 0 & 0 \\ 0 & 1 & 0 & 0 & 0 & 0 & 0 & 0 \\ 0 & 0 & 1 & 0 & 0 & 0 & 0 & 0 \\ 0 & 0 & 0 & 1 & 0 & 0 & 0 & 0 \\ 0 & 0 & 0 & 0 & 1 & 0 & 0 & 0 \\ 0 & 0 & 0 & 0 & 0 & 1 & 0 & 1 \\ 0 & 0 & 0 & 0 & 1 & 0 & 1 & 0 \\ 0 & 0 & 0 & 1 & 0 & 1 & 0 & 0 \\ 0 & 0 & 1 & 0 & 1 & 0 & 0 & 0 \\ 0 & 1 & 0 & 1 & 0 & 0 & 0 & 1 \\ 1 & 0 & 1 & 0 & 1 & 0 & 0 & 0 \\ 0 & 1 & 0 & 1 & 0 & 1 & 0 & 0 \\ 0 & 0 & 1 & 0 & 1 & 0 & 1 & 0 \\ 0 & 0 & 0 & 1 & 0 & 1 & 0 & 1 \\ 0 & 0 & 0 & 0 & 2 & 0 & 0 & 0 \\ 0 & 0 & 0 & 1 & 0 & 1 & 0 & 1 \\ 0 & 0 & 1 & 0 & 1 & 0 & 1 & 0 \\ 0 & 1 & 0 & 1 & 0 & 1 & 0 & 0 \\ 1 & 0 & 1 & 0 & 1 & 0 & 0 & 0 \\ 0 & 1 & 0 & 1 & 0 & 0 & 0 & 1 \\ 0 & 0 & 1 & 0 & 1 & 0 & 0 & 0 \\ 0 & 0 & 0 & 1 & 0 & 1 & 0 & 0 \\ 0 & 0 & 0 & 0 & 1 & 0 & 1 & 0 \\ 0 & 0 & 0 & 0 & 0 & 1 & 0 & 1 \\ 0 & 0 & 0 & 0 & 1 & 0 & 0 & 0 \\ 0 & 0 & 0 & 1 & 0 & 0 & 0 & 0 \\ 0 & 0 & 1 & 0 & 0 & 0 & 0 & 0 \\ 0 & 1 & 0 & 0 & 0 & 0 & 0 & 0 \\ 1 & 0 & 0 & 0 & 0 & 0 & 0 & 0 \end{pmatrix} \end{array}
 \end{array}$$

B Appendix B: Affine Adjacency Intertwiners

The adjacency matrix intertwiners C for the affine A - D - E models are as follows:

$$\begin{aligned}
 & A_{L-1}^{(1)}-D_{\frac{L}{2}+2}^{(1)} && A_5^{(1)}-E_6^{(1)} \\
 C = & \begin{pmatrix} 1 & 1 & 0 & \dots & 0 & 0 & 0 \\ 0 & 0 & 1 & \dots & 0 & 0 & 0 \\ \vdots & \vdots & \vdots & \ddots & \vdots & \vdots & \vdots \\ 0 & 0 & 0 & \dots & 1 & 0 & 0 \\ 0 & 0 & 0 & \dots & 0 & 1 & 1 \\ 0 & 0 & 0 & \dots & 1 & 0 & 0 \\ \vdots & \vdots & \vdots & \ddots & \vdots & \vdots & \vdots \\ 0 & 0 & 1 & \dots & 0 & 0 & 0 \end{pmatrix} && C = \begin{pmatrix} 0 & 1 & 0 & 0 & 0 & 1 & 0 \\ 1 & 0 & 1 & 0 & 0 & 0 & 0 \\ 0 & 1 & 0 & 1 & 0 & 0 & 0 \\ 0 & 0 & 1 & 0 & 1 & 0 & 0 \\ 0 & 0 & 0 & 1 & 0 & 1 & 0 \\ 0 & 0 & 1 & 0 & 0 & 0 & 1 \end{pmatrix} \\
 & A_7^{(1)}-E_7^{(1)} && A_9^{(1)}-E_8^{(1)} \\
 C = & \begin{pmatrix} 1 & 0 & 1 & 0 & 0 & 0 & 0 & 1 \\ 0 & 1 & 0 & 1 & 0 & 0 & 0 & 0 \\ 0 & 0 & 1 & 0 & 1 & 0 & 0 & 0 \\ 0 & 0 & 0 & 1 & 0 & 1 & 0 & 0 \\ 0 & 0 & 0 & 0 & 1 & 0 & 1 & 1 \\ 0 & 0 & 0 & 1 & 0 & 1 & 0 & 0 \\ 0 & 0 & 1 & 0 & 1 & 0 & 0 & 0 \\ 0 & 1 & 0 & 1 & 0 & 0 & 0 & 0 \end{pmatrix} && C = \begin{pmatrix} 1 & 0 & 1 & 0 & 1 & 0 & 0 & 0 & 1 \\ 0 & 1 & 0 & 1 & 0 & 1 & 0 & 0 & 0 \\ 0 & 0 & 1 & 0 & 1 & 0 & 1 & 0 & 0 \\ 0 & 0 & 0 & 1 & 0 & 1 & 0 & 1 & 0 \\ 0 & 0 & 0 & 0 & 1 & 0 & 1 & 0 & 1 \\ 0 & 0 & 0 & 0 & 0 & 2 & 0 & 0 & 0 \\ 0 & 0 & 0 & 0 & 1 & 0 & 1 & 0 & 1 \\ 0 & 0 & 0 & 1 & 0 & 1 & 0 & 1 & 0 \\ 0 & 0 & 1 & 0 & 1 & 0 & 1 & 0 & 0 \\ 0 & 1 & 0 & 1 & 0 & 1 & 0 & 0 & 0 \end{pmatrix}
 \end{aligned}$$

C Appendix C: Classical Cell Intertwiners

C.1 Nonzero Cells for the A_L - $D_{\frac{L+3}{2}}$ Intertwiner

$$\begin{aligned}
 & \begin{array}{c} i+1 \quad i+1 \\ \begin{array}{|c|c|} \hline \rightarrow & \rightarrow \\ \hline \end{array} \\ i \quad i \end{array} = \begin{array}{c} i \quad i \\ \begin{array}{|c|c|} \hline \rightarrow & \rightarrow \\ \hline \end{array} \\ i+1 \quad i+1 \end{array} = 1 \quad \text{for } i = 1, 2, \dots, (L-3)/2; \\
 & \begin{array}{c} L-i+1 \quad i+2 \\ \begin{array}{|c|c|} \hline \rightarrow & \rightarrow \\ \hline \end{array} \\ L-i \quad i+1 \end{array} = \begin{array}{c} L-i \quad i+1 \\ \begin{array}{|c|c|} \hline \rightarrow & \rightarrow \\ \hline \end{array} \\ L-i+1 \quad i+2 \end{array} = 1 \quad \text{for } i = 0, 1, \dots, (L-5)/2; \\
 & \begin{pmatrix} \begin{array}{c} \frac{L+1}{2} \quad \frac{L+1}{2} \\ \begin{array}{|c|c|} \hline \rightarrow & \rightarrow \\ \hline \end{array} \\ \frac{L-1}{2} \quad \frac{L-1}{2} \end{array} & \begin{array}{c} \frac{L+1}{2} \quad \frac{L+3}{2} \\ \begin{array}{|c|c|} \hline \rightarrow & \rightarrow \\ \hline \end{array} \\ \frac{L-1}{2} \quad \frac{L-1}{2} \end{array} \end{pmatrix} = \frac{1}{\sqrt{2}} \begin{pmatrix} 1 & -1 \\ 1 & 1 \end{pmatrix}; \\
 & \begin{pmatrix} \begin{array}{c} \frac{L+3}{2} \quad \frac{L-1}{2} \\ \begin{array}{|c|c|} \hline \rightarrow & \rightarrow \\ \hline \end{array} \\ \frac{L-1}{2} \quad \frac{L-1}{2} \end{array} & \begin{array}{c} \frac{L+3}{2} \quad \frac{L-1}{2} \\ \begin{array}{|c|c|} \hline \rightarrow & \rightarrow \\ \hline \end{array} \\ \frac{L-1}{2} \quad \frac{L-1}{2} \end{array} \end{pmatrix} = \begin{pmatrix} 1 & -1 \\ 1 & 1 \end{pmatrix}; \\
 & \begin{pmatrix} \begin{array}{c} \frac{L+1}{2} \quad \frac{L+1}{2} \\ \begin{array}{|c|c|} \hline \rightarrow & \rightarrow \\ \hline \end{array} \\ \frac{L+3}{2} \quad \frac{L-1}{2} \end{array} & \begin{array}{c} \frac{L+1}{2} \quad \frac{L+3}{2} \\ \begin{array}{|c|c|} \hline \rightarrow & \rightarrow \\ \hline \end{array} \\ \frac{L+3}{2} \quad \frac{L-1}{2} \end{array} \end{pmatrix} = \begin{pmatrix} 1 & -1 \\ 1 & 1 \end{pmatrix};
 \end{aligned}$$

$$\begin{pmatrix} \begin{array}{c} \begin{array}{cc} 9 & 1 \\ \downarrow & \rightarrow \\ 10 & 2 \end{array} & \begin{array}{cc} 9 & 3 \\ \downarrow & \rightarrow \\ 10 & 2 \end{array} \\ \begin{array}{cc} 9 & 1 \\ \downarrow & \rightarrow \\ 8 & 2 \end{array} & \begin{array}{cc} 9 & 3 \\ \downarrow & \rightarrow \\ 8 & 2 \end{array} \end{array} \right) = \begin{pmatrix} \cos m_6 & \sin m_6 \\ \sin m_6 & -\cos m_6 \end{pmatrix};$$

$$\begin{pmatrix} \begin{array}{c} \begin{array}{cc} 10 & 2 \\ \downarrow & \rightarrow \\ 11 & 3 \end{array} & \begin{array}{cc} 10 & 4 \\ \downarrow & \rightarrow \\ 11 & 3 \end{array} \\ \begin{array}{cc} 10 & 2 \\ \downarrow & \rightarrow \\ 9 & 3 \end{array} & \begin{array}{cc} 10 & 4 \\ \downarrow & \rightarrow \\ 9 & 3 \end{array} \end{array} \right) = \begin{pmatrix} \cos m_7 & -\sin m_7 \\ \sin m_7 & \cos m_7 \end{pmatrix};$$

$$\begin{pmatrix} \begin{array}{c} \begin{array}{cc} 11 & 3 \\ \downarrow & \rightarrow \\ 12 & 4 \end{array} & \begin{array}{cc} 11 & 5 \\ \downarrow & \rightarrow \\ 12 & 4 \end{array} \\ \begin{array}{cc} 11 & 3 \\ \downarrow & \rightarrow \\ 10 & 4 \end{array} & \begin{array}{cc} 11 & 5 \\ \downarrow & \rightarrow \\ 10 & 4 \end{array} \end{array} \right) = \begin{pmatrix} \sin m_3 & \cos m_3 \\ -\cos m_3 & \sin m_3 \end{pmatrix};$$

$$\begin{pmatrix} \begin{array}{c} \begin{array}{cc} 12 & 4 \\ \downarrow & \rightarrow \\ 13 & 5 \end{array} & \begin{array}{cc} 12 & 6 \\ \downarrow & \rightarrow \\ 13 & 5 \end{array} \\ \begin{array}{cc} 12 & 4 \\ \downarrow & \rightarrow \\ 11 & 5 \end{array} & \begin{array}{cc} 12 & 6 \\ \downarrow & \rightarrow \\ 11 & 5 \end{array} \end{array} \right) = \begin{pmatrix} -\sin m_2 & \cos m_2 \\ \cos m_2 & \sin m_2 \end{pmatrix};$$

$$\begin{pmatrix} \begin{array}{c} \begin{array}{cc} 13 & 7 \\ \downarrow & \rightarrow \\ 14 & 4 \end{array} & \begin{array}{cc} 13 & 5 \\ \downarrow & \rightarrow \\ 14 & 4 \end{array} \\ \begin{array}{cc} 13 & 7 \\ \downarrow & \rightarrow \\ 12 & 4 \end{array} & \begin{array}{cc} 13 & 5 \\ \downarrow & \rightarrow \\ 12 & 4 \end{array} \end{array} \right) = \begin{pmatrix} \sin m_1 & \cos m_1 \\ \cos m_1 & -\sin m_1 \end{pmatrix};$$

$$\begin{aligned} \sin m_1 &= \sqrt{\frac{S_7^A S_6^E}{S_5^A S_4^E}}; & \sin m_2 &= \sqrt{\frac{S_4^A S_7^E}{S_6^A S_5^E}}; \\ \cos m_3 &= \sqrt{\frac{S_5^A S_6^E}{S_7^A S_4^E}}; & \cos m_4 &= \sqrt{\frac{S_{10}^A S_1^E}{S_8^A S_3^E}}; \\ \sin m_5 &= \sqrt{\frac{S_7^A S_2^E}{S_9^A S_4^E}}; & \cos m_6 &= \sqrt{\frac{S_5^A S_6^E}{S_9^A S_2^E}}; \\ \cos m_7 &= \sqrt{\frac{S_8^A S_7^E}{S_{10}^A S_3^E}}. \end{aligned}$$

$$\begin{pmatrix} \begin{array}{ccc} \begin{array}{c} 14 \rightarrow 1 \rightarrow 8 \\ \downarrow \\ 13 \rightarrow 1 \rightarrow 5 \end{array} & \begin{array}{c} 14 \rightarrow 1 \rightarrow 6 \\ \downarrow \\ 13 \rightarrow 1 \rightarrow 5 \end{array} & \begin{array}{c} 14 \rightarrow 1 \rightarrow 4 \\ \downarrow \\ 13 \rightarrow 1 \rightarrow 5 \end{array} \\ \begin{array}{ccc} \begin{array}{c} 14 \rightarrow 1 \rightarrow 8 \\ \downarrow \\ 15 \rightarrow 1 \rightarrow 5 \end{array} & \begin{array}{c} 14 \rightarrow 1 \rightarrow 6 \\ \downarrow \\ 15 \rightarrow 1 \rightarrow 5 \end{array} & \begin{array}{c} 14 \rightarrow 1 \rightarrow 4 \\ \downarrow \\ 15 \rightarrow 1 \rightarrow 5 \end{array} \\ \begin{array}{ccc} \begin{array}{c} 14 \rightarrow 1 \rightarrow 8 \\ \downarrow \\ 15 \rightarrow 2 \rightarrow 5 \end{array} & \begin{array}{c} 14 \rightarrow 1 \rightarrow 6 \\ \downarrow \\ 15 \rightarrow 2 \rightarrow 5 \end{array} & \begin{array}{c} 14 \rightarrow 1 \rightarrow 4 \\ \downarrow \\ 15 \rightarrow 2 \rightarrow 5 \end{array} \end{array} \end{pmatrix} = \begin{pmatrix} a_3 & a_2 & a_1 \\ b_3 & b_2 & b_1 \\ c_3 & c_2 & c_1 \end{pmatrix};$$

$$\begin{pmatrix} \begin{array}{ccc} \begin{array}{c} 13 \rightarrow 1 \rightarrow 5 \\ \downarrow \\ 14 \rightarrow 1 \rightarrow 8 \end{array} & \begin{array}{c} 13 \rightarrow 1 \rightarrow 5 \\ \downarrow \\ 14 \rightarrow 1 \rightarrow 6 \end{array} & \begin{array}{c} 13 \rightarrow 1 \rightarrow 5 \\ \downarrow \\ 14 \rightarrow 1 \rightarrow 4 \end{array} \\ \begin{array}{ccc} \begin{array}{c} 15 \rightarrow 1 \rightarrow 5 \\ \downarrow \\ 14 \rightarrow 1 \rightarrow 8 \end{array} & \begin{array}{c} 15 \rightarrow 1 \rightarrow 5 \\ \downarrow \\ 14 \rightarrow 1 \rightarrow 6 \end{array} & \begin{array}{c} 15 \rightarrow 1 \rightarrow 5 \\ \downarrow \\ 14 \rightarrow 1 \rightarrow 4 \end{array} \\ \begin{array}{ccc} \begin{array}{c} 15 \rightarrow 2 \rightarrow 5 \\ \downarrow \\ 14 \rightarrow 1 \rightarrow 8 \end{array} & \begin{array}{c} 15 \rightarrow 2 \rightarrow 5 \\ \downarrow \\ 14 \rightarrow 1 \rightarrow 6 \end{array} & \begin{array}{c} 15 \rightarrow 2 \rightarrow 5 \\ \downarrow \\ 14 \rightarrow 1 \rightarrow 4 \end{array} \end{array} \end{pmatrix} = \begin{pmatrix} \bar{a}_3 & \bar{a}_2 & \bar{a}_1 \\ \bar{b}_3 & \bar{b}_2 & \bar{b}_1 \\ \bar{c}_3 & \bar{c}_2 & \bar{c}_1 \end{pmatrix};$$

$$\begin{pmatrix} \begin{array}{ccc} \begin{array}{c} 16 \rightarrow 1 \rightarrow 8 \\ \downarrow \\ 15 \rightarrow 2 \rightarrow 5 \end{array} & \begin{array}{c} 16 \rightarrow 1 \rightarrow 8 \\ \downarrow \\ 15 \rightarrow 1 \rightarrow 5 \end{array} \\ \begin{array}{ccc} \begin{array}{c} 16 \rightarrow 1 \rightarrow 6 \\ \downarrow \\ 15 \rightarrow 2 \rightarrow 5 \end{array} & \begin{array}{c} 16 \rightarrow 1 \rightarrow 6 \\ \downarrow \\ 15 \rightarrow 1 \rightarrow 5 \end{array} \\ \begin{array}{ccc} \begin{array}{c} 16 \rightarrow 1 \rightarrow 4 \\ \downarrow \\ 15 \rightarrow 2 \rightarrow 5 \end{array} & \begin{array}{c} 16 \rightarrow 1 \rightarrow 4 \\ \downarrow \\ 15 \rightarrow 1 \rightarrow 5 \end{array} \end{array} \end{pmatrix} = \begin{pmatrix} -b_3 & c_3 \\ -b_2 & c_2 \\ -b_1 & c_1 \end{pmatrix};$$

$$\begin{pmatrix} \begin{array}{ccc} \begin{array}{c} 15 \rightarrow 2 \rightarrow 5 \\ \downarrow \\ 16 \rightarrow 1 \rightarrow 8 \end{array} & \begin{array}{c} 15 \rightarrow 1 \rightarrow 5 \\ \downarrow \\ 16 \rightarrow 1 \rightarrow 8 \end{array} \\ \begin{array}{ccc} \begin{array}{c} 15 \rightarrow 2 \rightarrow 5 \\ \downarrow \\ 16 \rightarrow 1 \rightarrow 6 \end{array} & \begin{array}{c} 15 \rightarrow 1 \rightarrow 5 \\ \downarrow \\ 16 \rightarrow 1 \rightarrow 6 \end{array} \\ \begin{array}{ccc} \begin{array}{c} 15 \rightarrow 2 \rightarrow 5 \\ \downarrow \\ 16 \rightarrow 1 \rightarrow 4 \end{array} & \begin{array}{c} 15 \rightarrow 1 \rightarrow 5 \\ \downarrow \\ 16 \rightarrow 1 \rightarrow 4 \end{array} \end{array} \end{pmatrix} = \begin{pmatrix} -\bar{b}_3 & \bar{c}_3 \\ -\bar{b}_2 & \bar{c}_2 \\ -\bar{b}_1 & \bar{c}_1 \end{pmatrix};$$

$$\begin{aligned} a_1 &= \sin \gamma; & a_2 &= \cos \gamma \sin \alpha; \\ a_3 &= \cos \alpha \cos \gamma; & b_1 &= \cos \gamma \sin \beta; \\ b_2 &= \cos \alpha \cos \beta - \sin \alpha \sin \beta \sin \gamma; \\ b_3 &= -\cos \beta \sin \alpha - \cos \alpha \sin \beta \sin \gamma; \\ c_1 &= \cos \beta \cos \gamma; \\ c_2 &= -\cos \alpha \sin \beta - \cos \beta \sin \alpha \sin \gamma; \\ c_3 &= \sin \alpha \sin \beta - \cos \alpha \cos \beta \sin \gamma; \\ \bar{a}_1 &= \sin m_{12} = a_1 \sqrt{\frac{S_{14}^A S_5^E}{S_{13}^A S_4^E}}; \end{aligned}$$

$$\begin{aligned}
\bar{a}_3 &= a_3 \sqrt{\frac{S_{14}^A S_5^E}{S_{13}^A S_8^E}}; & \bar{a}_2 &= \cos m_{10} = a_2 \sqrt{\frac{S_{14}^A S_5^E}{S_{13}^A S_6^E}}; \\
\bar{b}_1 &= b_1 \sqrt{\frac{S_{14}^A S_5^E}{S_{15}^A S_4^E}}; & \bar{b}_2 &= b_2 \sqrt{\frac{S_{14}^A S_5^E}{S_{15}^A S_6^E}}; \\
\bar{b}_3 &= b_3 \sqrt{\frac{S_{14}^A S_5^E}{S_{15}^A S_8^E}}; & \bar{c}_1 &= c_1 \sqrt{\frac{S_{14}^A S_5^E}{S_{15}^A S_4^E}}; \\
\bar{c}_2 &= c_2 \sqrt{\frac{S_{14}^A S_5^E}{S_{15}^A S_6^E}}; & \bar{c}_3 &= c_3 \sqrt{\frac{S_{14}^A S_5^E}{S_{15}^A S_8^E}}; \\
\cos \gamma &= \sqrt{\frac{S_{15}^A S_4^E}{S_{14}^A S_5^E}}; & \sin \alpha &= \sin \alpha = \sqrt{\frac{S_{14}^A S_5^E - S_{15}^A S_6^E}{S_{15}^A S_4^E}}; \\
\sin m_1 &= \sqrt{\frac{S_8^A S_7^E}{S_6^A S_5^E}}; & \sin m_2 &= \sqrt{\frac{S_5^A S_8^E}{S_7^A S_6^E}}; \\
\cos m_3 &= \sqrt{\frac{S_6^A S_7^E}{S_8^A S_5^E}}; & \sin m_4 &= \sqrt{\frac{S_{11}^A S_8^E}{S_9^A S_4^E}}; \\
\cos m_5 &= \sqrt{\frac{S_{12}^A S_1^E}{S_{10}^A S_3^E}}; & \cos m_6 &= \sqrt{\frac{S_9^A S_4^E}{S_{11}^A S_2^E}} \sqrt{1 - \frac{S_{11}^A S_8^E}{S_9^A S_4^E}}; \\
\sin m_7 &= \sqrt{\frac{S_8^A S_3^E}{S_{10}^A S_5^E}}; & \sin m_8 &= \sqrt{\frac{S_9^A S_2^E}{S_{11}^A S_4^E}}; \\
\cos m_9 &= \sqrt{\frac{S_{14}^A S_3^E}{S_{12}^A S_5^E}}; & \sin m_{10} &= \sqrt{\frac{S_9^A S_2^E}{S_{11}^A S_4^E}} \sqrt{\frac{S_{11}^A S_4^E}{S_{13}^A S_6^E}}; \\
\sin m_{11} &= \sqrt{\frac{S_{10}^A S_1^E}{S_{12}^A S_3^E}}; & \sin m_{12} &= \sqrt{\frac{S_{11}^A S_2^E}{S_{13}^A S_4^E}} \sqrt{1 - \frac{S_9^A S_4^E}{S_{11}^A S_2^E} \left(1 - \frac{S_{11}^A S_8^E}{S_9^A S_4^E}\right)}.
\end{aligned}$$

D Appendix D: Affine Cell Intertwiners

D.1 Nonzero Cells for the $A_{L-1}^{(1)} - D_{\frac{L}{2}+2}^{(1)}$ Intertwiner

$$\begin{aligned}
\begin{array}{c} i+1 \longrightarrow i+2 \\ \downarrow \qquad \downarrow \\ i \longrightarrow i+1 \end{array} &= -1 \quad \text{for } i = 2, 3, \dots, \frac{L}{2} - 1; \\
\begin{array}{c} i \longrightarrow i+1 \\ \downarrow \qquad \downarrow \\ i+1 \longrightarrow i+2 \end{array} &= 1 \quad \text{for } i = 2, 3, \dots, \frac{L}{2} - 1; \\
\begin{array}{c} L-i+1 \longrightarrow i+2 \\ \downarrow \qquad \downarrow \\ L-i \longrightarrow i+3 \end{array} &= \begin{array}{c} L-i \longrightarrow i+3 \\ \downarrow \qquad \downarrow \\ L-i+1 \longrightarrow i+2 \end{array} = 1 \quad \text{for } i = 1, 2, \dots, \frac{L}{2} - 2;
\end{aligned}$$

$$\begin{pmatrix} \begin{array}{c} \begin{array}{cc} 4 \rightarrow 3 \\ \downarrow \quad \downarrow \\ 5 \rightarrow 4 \end{array} & \begin{array}{c} \begin{array}{cc} 4 \rightarrow 5 \\ \downarrow \quad \downarrow \\ 5 \rightarrow 4 \end{array} \\ \begin{array}{c} \begin{array}{cc} 4 \rightarrow 3 \\ \downarrow \quad \downarrow \\ 3 \rightarrow 4 \end{array} & \begin{array}{c} \begin{array}{cc} 4 \rightarrow 5 \\ \downarrow \quad \downarrow \\ 3 \rightarrow 4 \end{array} \end{array} \end{pmatrix} = \begin{pmatrix} -\cos m_3 & \sin m_3 \\ \sin m_3 & \cos m_3 \end{pmatrix};$$

$$\begin{pmatrix} \begin{array}{c} \begin{array}{cc} 5 \rightarrow 6 \\ \downarrow \quad \downarrow \\ 6 \rightarrow 3 \end{array} & \begin{array}{c} \begin{array}{cc} 5 \rightarrow 4 \\ \downarrow \quad \downarrow \\ 6 \rightarrow 3 \end{array} \\ \begin{array}{c} \begin{array}{cc} 5 \rightarrow 6 \\ \downarrow \quad \downarrow \\ 4 \rightarrow 3 \end{array} & \begin{array}{c} \begin{array}{cc} 5 \rightarrow 4 \\ \downarrow \quad \downarrow \\ 4 \rightarrow 3 \end{array} \end{array} \end{pmatrix} = \begin{pmatrix} \cos m_4 & \sin m_4 \\ \sin m_4 & -\cos m_4 \end{pmatrix};$$

$$\begin{pmatrix} \begin{array}{c} \begin{array}{cc} 6 \rightarrow 7 \\ \downarrow \quad \downarrow \\ 1 \rightarrow 6 \end{array} & \begin{array}{c} \begin{array}{cc} 6 \rightarrow 3 \\ \downarrow \quad \downarrow \\ 1 \rightarrow 6 \end{array} \\ \begin{array}{c} \begin{array}{cc} 6 \rightarrow 7 \\ \downarrow \quad \downarrow \\ 5 \rightarrow 6 \end{array} & \begin{array}{c} \begin{array}{cc} 6 \rightarrow 3 \\ \downarrow \quad \downarrow \\ 5 \rightarrow 6 \end{array} \end{array} \end{pmatrix} = \begin{pmatrix} \cos m_5 & -\sin m_5 \\ \sin m_5 & \cos m_5 \end{pmatrix};$$

$$\begin{pmatrix} \begin{array}{c} \begin{array}{cc} 1 \rightarrow 6 \\ \downarrow \quad \downarrow \\ 2 \rightarrow 3 \end{array} & \begin{array}{c} \begin{array}{cc} 1 \rightarrow 2 \\ \downarrow \quad \downarrow \\ 2 \rightarrow 3 \end{array} \\ \begin{array}{c} \begin{array}{cc} 1 \rightarrow 6 \\ \downarrow \quad \downarrow \\ 6 \rightarrow 3 \end{array} & \begin{array}{c} \begin{array}{cc} 1 \rightarrow 2 \\ \downarrow \quad \downarrow \\ 6 \rightarrow 3 \end{array} \end{array} \end{pmatrix} = \begin{pmatrix} \cos m_6 & \sin m_6 \\ -\sin m_6 & \cos m_6 \end{pmatrix};$$

$$\begin{aligned} \sin m_1 &= \sqrt{\frac{S_1^E}{S_2^E}}; & \sin m_2 &= \sqrt{\frac{S_5^E}{S_3^E}}; & \sin m_3 &= \sqrt{\frac{S_5^E}{S_4^E}}; \\ \cos m_4 &= \sqrt{\frac{S_7^E}{S_3^E}}; & \sin m_5 &= \sqrt{\frac{S_7^E}{S_6^E}}; & \sin m_6 &= \sqrt{\frac{S_1^E}{S_3^E}}; \end{aligned}$$

D.3 Nonzero Cells for the $A_7^{(1)} - E_7^{(1)}$ Intertwiner

$$\begin{aligned} \begin{array}{c} \begin{array}{cc} 2 \rightarrow 2 \\ \downarrow \quad \downarrow \\ 1 \rightarrow 1 \end{array} &= \begin{array}{c} \begin{array}{cc} 3 \rightarrow 3 \\ \downarrow \quad \downarrow \\ 2 \rightarrow 2 \end{array} &= \begin{array}{c} \begin{array}{cc} 4 \rightarrow 4 \\ \downarrow \quad \downarrow \\ 3 \rightarrow 3 \end{array} &= \begin{array}{c} \begin{array}{cc} 4 \rightarrow 4 \\ \downarrow \quad \downarrow \\ 5 \rightarrow 8 \end{array} &= \begin{array}{c} \begin{array}{cc} 6 \rightarrow 4 \\ \downarrow \quad \downarrow \\ 5 \rightarrow 8 \end{array} &= \begin{array}{c} \begin{array}{cc} 6 \rightarrow 4 \\ \downarrow \quad \downarrow \\ 7 \rightarrow 3 \end{array} \\ \begin{array}{c} \begin{array}{cc} 7 \rightarrow 3 \\ \downarrow \quad \downarrow \\ 8 \rightarrow 2 \end{array} &= \begin{array}{c} \begin{array}{cc} 8 \rightarrow 2 \\ \downarrow \quad \downarrow \\ 1 \rightarrow 1 \end{array} &= \begin{array}{c} \begin{array}{cc} 8 \rightarrow 4 \\ \downarrow \quad \downarrow \\ 1 \rightarrow 8 \end{array} &= \begin{array}{c} \begin{array}{cc} 2 \rightarrow 4 \\ \downarrow \quad \downarrow \\ 1 \rightarrow 8 \end{array} &= \begin{array}{c} \begin{array}{cc} 2 \rightarrow 4 \\ \downarrow \quad \downarrow \\ 3 \rightarrow 5 \end{array} &= \begin{array}{c} \begin{array}{cc} 3 \rightarrow 5 \\ \downarrow \quad \downarrow \\ 4 \rightarrow 6 \end{array} \\ \begin{array}{c} \begin{array}{cc} 4 \rightarrow 6 \\ \downarrow \quad \downarrow \\ 5 \rightarrow 7 \end{array} &= \begin{array}{c} \begin{array}{cc} 6 \rightarrow 6 \\ \downarrow \quad \downarrow \\ 5 \rightarrow 7 \end{array} &= \begin{array}{c} \begin{array}{cc} 7 \rightarrow 5 \\ \downarrow \quad \downarrow \\ 6 \rightarrow 6 \end{array} &= \begin{array}{c} \begin{array}{cc} 8 \rightarrow 4 \\ \downarrow \quad \downarrow \\ 7 \rightarrow 5 \end{array} &= 1; \end{array} \end{aligned}$$

$$\begin{pmatrix} \begin{array}{c} \begin{array}{cc} 2 \rightarrow 2 \\ \downarrow \quad \downarrow \\ 1 \rightarrow 3 \end{array} & \begin{array}{c} \begin{array}{cc} 2 \rightarrow 4 \\ \downarrow \quad \downarrow \\ 1 \rightarrow 3 \end{array} \\ \begin{array}{c} \begin{array}{cc} 2 \rightarrow 2 \\ \downarrow \quad \downarrow \\ 3 \rightarrow 3 \end{array} & \begin{array}{c} \begin{array}{cc} 2 \rightarrow 4 \\ \downarrow \quad \downarrow \\ 3 \rightarrow 3 \end{array} \end{array} \end{pmatrix} = \begin{pmatrix} -\sin m_1 & -\cos m_1 \\ \cos m_1 & -\sin m_1 \end{pmatrix};$$

$$\begin{pmatrix} \begin{array}{c} \begin{array}{ccc} 1 & \rightarrow & 3 \\ \downarrow & & \downarrow \\ 8 & \rightarrow & 4 \end{array} & \begin{array}{ccc} 1 & \rightarrow & 8 \\ \downarrow & & \downarrow \\ 8 & \rightarrow & 4 \end{array} \\ \begin{array}{ccc} 1 & \rightarrow & 3 \\ \downarrow & & \downarrow \\ 2 & \rightarrow & 4 \end{array} & \begin{array}{ccc} 1 & \rightarrow & 8 \\ \downarrow & & \downarrow \\ 2 & \rightarrow & 4 \end{array} \end{array} \right) = \begin{pmatrix} \sin m_0 & \cos m_0 \\ -\cos m_0 & \sin m_0 \end{pmatrix};$$

$$\begin{aligned} \cos m_0 &= \sqrt{\frac{S_2^E}{S_4^E}}; & \cos m_1 &= \sqrt{\frac{S_2^E}{S_3^E}}; & \cos m_2 &= \sqrt{\frac{S_5^E}{S_4^E}}; \\ \cos m_3 &= \sqrt{\frac{S_6^E}{S_5^E}}; & \cos m_4 &= \sqrt{\frac{S_7^E}{S_6^E}}; & \sin m_5 &= \sqrt{\frac{S_6^E}{S_5^E}}; \\ \sin m_6 &= \sqrt{\frac{S_5^E}{S_4^E}}; & \sin m_7 &= \sqrt{\frac{S_2^E}{S_3^E}}; & \cos m_8 &= \sqrt{\frac{S_1^E}{S_2^E}}; \\ \sin m_9 &= \sqrt{\frac{S_8^E}{S_4^E}}; \end{aligned}$$

D.4 Nonzero Cells for the $A_9^{(1)} - E_8^{(1)}$ Intertwiner

$$\begin{aligned} \begin{array}{c} \begin{array}{ccc} 10 & \rightarrow & 2 \\ \downarrow & & \downarrow \\ 1 & \rightarrow & 1 \end{array} & = & \begin{array}{ccc} 3 & \rightarrow & 3 \\ \downarrow & & \downarrow \\ 2 & \rightarrow & 2 \end{array} & = & \begin{array}{ccc} 4 & \rightarrow & 4 \\ \downarrow & & \downarrow \\ 3 & \rightarrow & 3 \end{array} & = & \begin{array}{ccc} 5 & \rightarrow & 5 \\ \downarrow & & \downarrow \\ 4 & \rightarrow & 4 \end{array} & = & \begin{array}{ccc} 10 & \rightarrow & 6 \\ \downarrow & & \downarrow \\ 1 & \rightarrow & 9 \end{array} & = & \begin{array}{ccc} 2 & \rightarrow & 6 \\ \downarrow & & \downarrow \\ 1 & \rightarrow & 9 \end{array} & = & \begin{array}{ccc} 2 & \rightarrow & 6 \\ \downarrow & & \downarrow \\ 3 & \rightarrow & 7 \end{array} \\ \begin{array}{ccc} 3 & \rightarrow & 7 \\ \downarrow & & \downarrow \\ 4 & \rightarrow & 8 \end{array} & = & \begin{array}{ccc} 5 & \rightarrow & 7 \\ \downarrow & & \downarrow \\ 4 & \rightarrow & 8 \end{array} & = & \begin{array}{ccc} 7 & \rightarrow & 5 \\ \downarrow & & \downarrow \\ 8 & \rightarrow & 4 \end{array} & = & \begin{array}{ccc} 7 & \rightarrow & 7 \\ \downarrow & & \downarrow \\ 8 & \rightarrow & 8 \end{array} & = & \begin{array}{ccc} 10 & \rightarrow & 6 \\ \downarrow & & \downarrow \\ 9 & \rightarrow & 7 \end{array} & = & \begin{array}{ccc} 9 & \rightarrow & 3 \\ \downarrow & & \downarrow \\ 10 & \rightarrow & 2 \end{array} & = & 1; \\ \begin{array}{ccc} 2 & \rightarrow & 2 \\ \downarrow & & \downarrow \\ 1 & \rightarrow & 1 \end{array} & = & \begin{array}{ccc} 9 & \rightarrow & 7 \\ \downarrow & & \downarrow \\ 8 & \rightarrow & 8 \end{array} & = & \begin{array}{ccc} 8 & \rightarrow & 4 \\ \downarrow & & \downarrow \\ 9 & \rightarrow & 3 \end{array} & = & -1; \end{aligned}$$

$$\begin{pmatrix} \begin{array}{ccc} 2 & \rightarrow & 2 \\ \downarrow & & \downarrow \\ 1 & \rightarrow & 3 \end{array} & \begin{array}{ccc} 2 & \rightarrow & 4 \\ \downarrow & & \downarrow \\ 1 & \rightarrow & 3 \end{array} \\ \begin{array}{ccc} 2 & \rightarrow & 2 \\ \downarrow & & \downarrow \\ 3 & \rightarrow & 3 \end{array} & \begin{array}{ccc} 2 & \rightarrow & 4 \\ \downarrow & & \downarrow \\ 3 & \rightarrow & 3 \end{array} \end{pmatrix} = \begin{pmatrix} -\sin m_1 & \cos m_1 \\ \cos m_1 & \sin m_1 \end{pmatrix};$$

$$\begin{pmatrix} \begin{array}{ccc} 3 & \rightarrow & 3 \\ \downarrow & & \downarrow \\ 2 & \rightarrow & 4 \end{array} & \begin{array}{ccc} 3 & \rightarrow & 5 \\ \downarrow & & \downarrow \\ 2 & \rightarrow & 4 \end{array} \\ \begin{array}{ccc} 3 & \rightarrow & 3 \\ \downarrow & & \downarrow \\ 4 & \rightarrow & 4 \end{array} & \begin{array}{ccc} 3 & \rightarrow & 5 \\ \downarrow & & \downarrow \\ 4 & \rightarrow & 4 \end{array} \end{pmatrix} = \begin{pmatrix} \sin m_2 & \cos m_2 \\ \cos m_2 & -\sin m_2 \end{pmatrix};$$

$$\begin{pmatrix} \begin{array}{ccc} \begin{array}{c} 4 \rightarrow 1 \rightarrow 6 \\ \downarrow \quad \downarrow \\ 5 \rightarrow 1 \rightarrow 9 \end{array} & \begin{array}{c} 4 \rightarrow 1 \rightarrow 6 \\ \downarrow \quad \downarrow \\ 5 \rightarrow 1 \rightarrow 7 \end{array} & \begin{array}{c} 4 \rightarrow 1 \rightarrow 6 \\ \downarrow \quad \downarrow \\ 5 \rightarrow 1 \rightarrow 5 \end{array} \\ \begin{array}{c} 6 \rightarrow 1 \rightarrow 6 \\ \downarrow \quad \downarrow \\ 5 \rightarrow 1 \rightarrow 9 \end{array} & \begin{array}{c} 6 \rightarrow 1 \rightarrow 6 \\ \downarrow \quad \downarrow \\ 5 \rightarrow 1 \rightarrow 7 \end{array} & \begin{array}{c} 6 \rightarrow 1 \rightarrow 6 \\ \downarrow \quad \downarrow \\ 5 \rightarrow 1 \rightarrow 5 \end{array} \\ \begin{array}{c} 6 \rightarrow 2 \rightarrow 6 \\ \downarrow \quad \downarrow \\ 5 \rightarrow 1 \rightarrow 9 \end{array} & \begin{array}{c} 6 \rightarrow 2 \rightarrow 6 \\ \downarrow \quad \downarrow \\ 5 \rightarrow 1 \rightarrow 7 \end{array} & \begin{array}{c} 6 \rightarrow 2 \rightarrow 6 \\ \downarrow \quad \downarrow \\ 5 \rightarrow 1 \rightarrow 5 \end{array} \end{array} \right) = \begin{pmatrix} \bar{a}_3 & \bar{a}_2 & \bar{a}_1 \\ \bar{b}_3 & \bar{b}_2 & \bar{b}_1 \\ \bar{c}_3 & \bar{c}_2 & \bar{c}_1 \end{pmatrix};$$

$$\begin{pmatrix} \begin{array}{ccc} \begin{array}{c} 7 \rightarrow 1 \rightarrow 9 \\ \downarrow \quad \downarrow \\ 8 \rightarrow 1 \rightarrow 6 \end{array} & \begin{array}{c} 7 \rightarrow 1 \rightarrow 7 \\ \downarrow \quad \downarrow \\ 8 \rightarrow 1 \rightarrow 6 \end{array} & \begin{array}{c} 7 \rightarrow 1 \rightarrow 5 \\ \downarrow \quad \downarrow \\ 8 \rightarrow 1 \rightarrow 6 \end{array} \\ \begin{array}{c} 7 \rightarrow 1 \rightarrow 9 \\ \downarrow \quad \downarrow \\ 6 \rightarrow 1 \rightarrow 6 \end{array} & \begin{array}{c} 7 \rightarrow 1 \rightarrow 7 \\ \downarrow \quad \downarrow \\ 6 \rightarrow 1 \rightarrow 6 \end{array} & \begin{array}{c} 7 \rightarrow 1 \rightarrow 5 \\ \downarrow \quad \downarrow \\ 6 \rightarrow 1 \rightarrow 6 \end{array} \\ \begin{array}{c} 7 \rightarrow 1 \rightarrow 9 \\ \downarrow \quad \downarrow \\ 6 \rightarrow 2 \rightarrow 6 \end{array} & \begin{array}{c} 7 \rightarrow 1 \rightarrow 7 \\ \downarrow \quad \downarrow \\ 6 \rightarrow 2 \rightarrow 6 \end{array} & \begin{array}{c} 7 \rightarrow 1 \rightarrow 5 \\ \downarrow \quad \downarrow \\ 6 \rightarrow 2 \rightarrow 6 \end{array} \end{array} \right) = \begin{pmatrix} a_3 & a_2 & a_1 \\ -b_3 & -b_2 & -b_1 \\ c_3 & c_2 & c_1 \end{pmatrix};$$

$$\begin{pmatrix} \begin{array}{ccc} \begin{array}{c} 8 \rightarrow 1 \rightarrow 6 \\ \downarrow \quad \downarrow \\ 7 \rightarrow 1 \rightarrow 9 \end{array} & \begin{array}{c} 8 \rightarrow 1 \rightarrow 6 \\ \downarrow \quad \downarrow \\ 7 \rightarrow 1 \rightarrow 7 \end{array} & \begin{array}{c} 8 \rightarrow 1 \rightarrow 6 \\ \downarrow \quad \downarrow \\ 7 \rightarrow 1 \rightarrow 5 \end{array} \\ \begin{array}{c} 6 \rightarrow 1 \rightarrow 6 \\ \downarrow \quad \downarrow \\ 7 \rightarrow 1 \rightarrow 9 \end{array} & \begin{array}{c} 6 \rightarrow 1 \rightarrow 6 \\ \downarrow \quad \downarrow \\ 7 \rightarrow 1 \rightarrow 7 \end{array} & \begin{array}{c} 6 \rightarrow 1 \rightarrow 6 \\ \downarrow \quad \downarrow \\ 7 \rightarrow 1 \rightarrow 5 \end{array} \\ \begin{array}{c} 6 \rightarrow 2 \rightarrow 6 \\ \downarrow \quad \downarrow \\ 7 \rightarrow 1 \rightarrow 9 \end{array} & \begin{array}{c} 6 \rightarrow 2 \rightarrow 6 \\ \downarrow \quad \downarrow \\ 7 \rightarrow 1 \rightarrow 7 \end{array} & \begin{array}{c} 6 \rightarrow 2 \rightarrow 6 \\ \downarrow \quad \downarrow \\ 7 \rightarrow 1 \rightarrow 5 \end{array} \end{array} \right) = \begin{pmatrix} \bar{a}_3 & \bar{a}_2 & \bar{a}_1 \\ -\bar{b}_3 & -\bar{b}_2 & -\bar{b}_1 \\ \bar{c}_3 & \bar{c}_2 & \bar{c}_1 \end{pmatrix};$$

$$\begin{aligned} a_1 &= \sin \gamma; \\ a_2 &= \cos \gamma \sin \alpha; \\ a_3 &= \cos \alpha \cos \gamma; \\ b_1 &= \cos \gamma \sin \beta; \\ b_2 &= \cos \alpha \cos \beta - \sin \alpha \sin \beta \sin \gamma; \\ b_3 &= -\cos \beta \sin \alpha - \cos \alpha \sin \beta \sin \gamma; \\ c_1 &= \cos \beta \cos \gamma; \\ c_2 &= -\cos \alpha \sin \beta - \cos \beta \sin \alpha \sin \gamma; \\ c_3 &= \sin \alpha \sin \beta - \cos \alpha \cos \beta \sin \gamma; \end{aligned}$$

$$\bar{a}_1 = \sin m_3 = a_1 \sqrt{\frac{S_6^E}{S_5^E}};$$

$$\bar{a}_3 = a_3 \sqrt{\frac{S_6^E}{S_9^E}}; \quad \bar{a}_2 = \cos m_6 = a_2 \sqrt{\frac{S_6^E}{S_7^E}};$$

$$\bar{b}_1 = b_1 \sqrt{\frac{S_6^E}{S_5^E}}; \quad \bar{b}_2 = b_2 \sqrt{\frac{S_6^E}{S_7^E}};$$

$$\begin{aligned}
\bar{b}_3 &= b_3 \sqrt{\frac{S_6^E}{S_9^E}}; & \bar{c}_1 &= c_1 \sqrt{\frac{S_6^E}{S_5^E}}; \\
\bar{c}_2 &= c_2 \sqrt{\frac{S_6^E}{S_7^E}}; & \bar{c}_3 &= c_3 \sqrt{\frac{S_6^E}{S_9^E}}; \\
\cos \gamma &= \sqrt{\frac{S_5^E}{S_6^E}}; & \sin \alpha = \sin \beta &= \sqrt{\frac{S_6^E - S_7^E}{S_5^E}}; \\
\sin m_1 &= \sqrt{\frac{S_1^E}{S_3^E}}; & \cos m_2 &= \sqrt{\frac{S_3^E}{S_4^E}}; & \cos m_3 &= \sqrt{\frac{S_4^E}{S_5^E}}; \\
\cos m_4 &= \sqrt{\frac{S_3^E}{S_5^E}}; & \sin m_5 &= \sqrt{\frac{S_8^E}{S_6^E}}; & \sin m_6 &= \sqrt{\frac{S_8^E}{S_7^E}}; \\
\cos m_7 &= \sqrt{\frac{S_1^E}{S_2^E}}; & \sin m_8 &= \sqrt{\frac{S_2^E}{S_4^E}}; & \cos m_9 &= \sqrt{\frac{S_9^E}{S_6^E}};
\end{aligned}$$

References

1. A. Ocneanu, “Quantized Groups, String Algebras and Galois Theory for Algebras in Operator Algebras and Applications”, Lond. Math. Soc. Lecture Note Series **136**.
2. V. Pasquier, Commun. Math. Phys. **118** (1988) 335.
3. Ph. Roche, Commun. Math. Phys. **127** (1990) 395.
4. P. Di Francesco and J. B. Zuber, Nucl. Phys. **B338** (1990) 602.
5. V. Pasquier, Nucl. Phys. **B28** (1987) 162; J. Phys. A **20** (1987) L1229, 5707.
6. A. L. Owczarek and R. J. Baxter, J. Stat. Phys. **49** (1987) 1093.
7. R. Rietman, J. Phys. A **24** (1991) L1125–8.
8. P. Ginsparg, Nucl. Phys. **B295** [FS21] (1988) 153.
9. P. A. Pearce, Int. J. Mod. Phys. **B4** (1990) 715.
10. S. O. Warnaar, B. Nienhuis and K. A. Seaton, Phys. Rev. Lett. **69** (1992) 710.
11. Ph. Roche, Phys. Lett. **B4** (1992) 929.
12. R. J. Baxter, “Exactly Solved Models in Statistical Mechanics”, Academic Press, London, 1982.
13. G. E. Andrews, R. J. Baxter and P. J. Forrester, J. Stat. Phys. **35** (1984) 193.
14. C. N. Yang, Phys. Rev. Lett. **19** (1967) 1312.

15. P. A. Pearce and K. A. Seaton, Phys. Rev. Lett. **60** (1988) 1347; Ann. Phys. (N.Y) **193** (1989) 326.
16. A. Kuniba and T. Yajima, J. Stat. Phys. **52** (1988) 829.
17. E. Date, M. Jimbo, A. Kuniba, T. Miwa and M. Okado, Nucl. Phys. **B290** (1987) 231.
18. E. Date, M. Jimbo, A. Kuniba, T. Miwa and M. Okado, Adv. Stud. Pure Math., **16** (1988) 17.
19. V. V. Bazhanov and N. Yu Reshetikhin, Int. J. Mod. Phys. B **4** (1989) 115.
20. A. Klümper and P. A. Pearce, Physica A **183** (1992) 304.
21. P. A. Pearce, Int. J. Mod. Phys. **A7** Suppl. 1B (1992) 791.
22. P. Fendley and P. Ginsparg, Nucl. Phys. **B324** (1989) 549.
23. D. Gepner and Z. Qiu, Nucl. Phys. **B285** (1987) 423.
24. R. Kedem and B. M. McCoy, Construction of modular branching functions from Bethe's equations in the 3-state Potts chain, these proceedings (1993).
25. Y-K. Zhou and P. A. Pearce, Fusion of $A-D-E$ lattice models, in preparation (1993).